NUREG/CR-6878
ANL-03/35

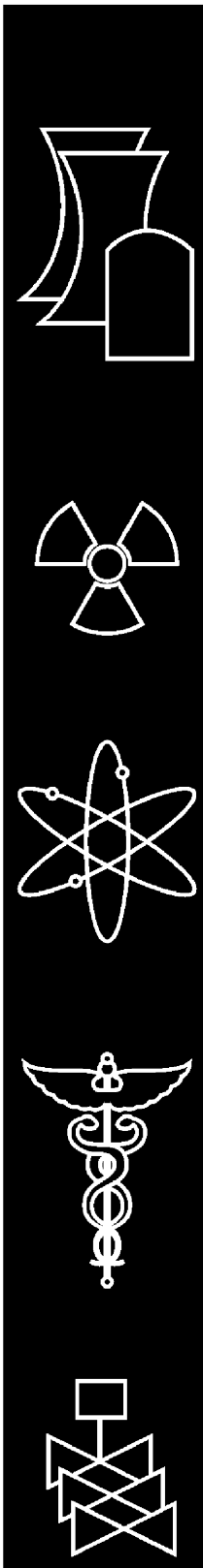

Effect of Material Heat Treatment on Fatigue Crack Initiation in Austenitic Stainless Steels in LWR Environments

Argonne National Laboratory

U.S. Nuclear Regulatory Commission
Office of Nuclear Regulatory Research
Washington, DC 20555-0001

NUREG/CR-6878
ANL-03/35

Effect of Material Heat Treatment on Fatigue Crack Initiation in Austenitic Stainless Steels in LWR Environments

Manuscript Completed: December 2003
Date Published: July 2005

Prepared by
O. K. Chopra, B. Alexandreanu, and W. J. Shack

Argonne National Laboratory
9700 South Cass Avenue
Argonne, IL 60439

W. H. Cullen, Jr., NRC Project Manager

Prepared for
Division of Engineering Technology
Office of Nuclear Regulatory Research
U.S. Nuclear Regulatory Commission
Washington, DC 20555-0001
NRC Job Code Y6388

Abstract

The ASME Boiler and Pressure Vessel Code provides rules for the design of Class 1 components of nuclear power plants. Figures I–9.1 through I–9.6 of Appendix I to Section III of the Code specify design curves for applicable structural materials. However, the effects of light water reactor (LWR) coolant environments are not explicitly addressed by the Code design curves. The existing fatigue strain–vs.–life (ε–N) data illustrate potentially significant effects of LWR coolant environments on the fatigue resistance of pressure vessel and piping steels. Under certain environmental and loading conditions, fatigue lives of austenitic stainless steels (SSs) can be a factor of 20 lower in water than in air. This report presents experimental data on the effect of heat treatment on fatigue crack initiation in austenitic Type 304 SS in LWR coolant environments. A detailed metallographic examination of fatigue test specimens was performed to characterize the crack morphology and fracture morphology. The key material, loading, and environmental parameters and their effect on the fatigue life of these steels are also described. Statistical models are presented for estimating the fatigue ε–N curves for austenitic SSs as a function of material, loading, and environmental parameters. Two methods for incorporating the effects of LWR coolant environments into the ASME Code fatigue evaluations are presented.

Foreword

This report examines the effects of various heat treatments and product forms (cast, welded or wrought) on the fatigue life of austenitic stainless steels (SSs) in light water reactor (LWR) environments. This report is one of a series dating back more than two decades, which has become increasingly relevant as licensees look forward to license renewal. This NUREG/CR report updates information presented in earlier reports by O. K. Chopra and his Argonne National Laboratory colleagues. The earlier reports include NUREG/CR-5704, Effects of LWR Coolant Environments on Fatigue Design Curves of Austenitic Stainless Steels; NUREG/CR-6717, Environmental Effects on Fatigue Crack Initiation in Piping and Pressure Vessel Steels; and, NUREG/CR-6787, Mechanism and Estimation of Fatigue Crack Initiation in Austenitic Stainless Steels in LWR Environments. The specific objective of this NUREG/CR is to present and discuss the effects of heat treatment on the fatigue life of stainless steels. Secondly, this test program takes advantage of improvements in test technique leading to more accurate data quality. Research such as reported here is required to support the realistic analysis of fatigue life of reactor components subjected to coolant environments and of cyclic changes in strain due to dead weight, thermal environment, and operating stresses.

Data from this research will be used to define the design curves in the ASME code or its equivalent. The data from this research and other published sources indicate that the existing code curves are non-conservative for austenitic stainless steels 304, 316 and 316NG. However, because of significant conservatism in quantifying other plant-related variables (such as the cyclic behavior, including stress and loading rates) involved in cumulative fatigue life calculations, the design of the current fleet of reactors is satisfactory, and the plants are safe to operate. The root of the problem with the realism of the code curves lies not in uncertainty about the degree of environmental degradation in specific environments or under specific heat treatments, but in the set of air environment results which were generated almost 30years ago and which serve as the basis for the stainless steel design curves. The air environment results are now known to be non-conservative and non-representative of most of the stainless steels used in actual nuclear component applications. The sources of the discrepancy reside in the specific choice of materials, test techniques and data analysis methods that were common practice when the database of air environment curves was developed more than forty years ago. Better specimen designs, improved test practices, and a better understanding of degradation mechanisms have produced a revised air environment baseline for stainless steels - one which is lower than the baseline which is now codified. The database described in this and earlier reports reinforces the NRC position that the design curves for the fatigue life of pressure boundary and internal components fabricated from stainless steel need revision. Several groups, including Argonne authors, a group of Japanese researchers, and the staff at Bettis Atomic Power Laboratory have proposed methods of establishing reference curves and safety factors for evaluation of the fatigue life of reactor components exposed to light-water reactor coolants and operational experience. This report presents a useful review of each of those proposed methods.

_____

Carl J. Paperiello, Director
Office of Nuclear Regulatory Research

Contents

Figures

Tables

Executive Summary

Section III, Subsection NB, of the ASME Boiler and Pressure Vessel Code contains rules for the design of Class 1 components of nuclear power plants. Figures I–9.1 through I–9.6 of Appendix I to Section III specify the Code design fatigue curves for applicable structural materials. However, Section III, Subsection NB–3121 of the Code states that effects of the coolant environment on fatigue resistance of a material were not intended to be addressed in these design curves. Therefore, the effects of environment on fatigue resistance of materials used in operating pressurized water reactor (PWR) and boiling water reactor (BWR) plants, whose primary–coolant pressure boundary components were designed in accordance with the Code, are uncertain.

The current Section–III design fatigue curves of the ASME Code were based primarily on strain–controlled fatigue tests of small polished specimens at room temperature in air. Best–fit curves to the experimental test data were first adjusted to account for the effects of mean stress and then lowered by a factor of 2 on stress and 20 on cycles (whichever was more conservative) to obtain the design fatigue curves. These factors are not safety margins but rather adjustment factors that must be applied to experimental data to obtain estimates of the lives of components. They were not intended to address the effects of the coolant environment on fatigue life. Recent fatigue–strain–vs.–life (ε–N) data obtained in the U.S. and Japan demonstrate that light water reactor (LWR) environments can have potentially significant effects on the fatigue resistance of materials. Specimen lives obtained from tests in simulated LWR environments can be much shorter than those obtained from corresponding tests in air.

This report presents experimental data on the effect of heat treatment on fatigue crack initiation in austenitic Type 304 stainless steel (SS) in LWR coolant environments. Fatigue tests have been conducted on two heats of Type 304 SS under various material conditions to determine the effect of heat treatment on fatigue crack initiation in these steels in air and LWR environments. A detailed metallographic examination of fatigue test specimens was performed, with special attention on crack morphology at the sites of initiation, the fracture surface, and the occurrence of striations.

Available fatigue ε–N data for wrought and cast austenitic SSs in air and LWR environments are reviewed, and statistical models that describe the effects of material and loading variables, such as steel type, strain amplitude, strain rate, temperature, dissolved oxygen (DO) level in water, surface roughness, and heat treatment on the fatigue lives of austenitic SSs are developed.

The new experimental data indicate that heat treatment has little or no effect on the fatigue life of Type 304 SS in air and low–DO PWR environments. In a high–DO BWR environment, fatigue life is lower for sensitized SSs; the decrease in life appears to increase as degree of sensitization is increased. The cyclic strain–hardening behavior of Type 304 SS under various heat treatment conditions is identical, only the fatigue life varies in environments that differ.

In air, irrespective of the degree of sensitization, the fracture mode for crack initiation (crack lengths up to ≈200 μm) and crack propagation (crack lengths >200 μm) is transgranular (TG), most likely along crystallographic planes, leaving behind relatively smooth facets. With increasing degree of sensitization, cleavage–like or stepped TG fracture, and, occasionally, ridge structures on the smooth surfaces were observed. In the BWR environment, the initial crack appeared intergranular (IG) for all heat treatment conditions, implying a weakening of the grain boundaries. For all four tested conditions, the initial IG mode transformed within 200 μm into a TG mode with cleavage–like features. It appears, however, that the size of the IG portion of the crack surface increased with the degree of sensitization. By

contrast, for all samples tested in PWR environments, the cracks initiated and propagated in a TG mode irrespective of the degree of sensitization. Prominent features of all fracture surfaces in the PWR case were highly angular, cleavage–like fracture facets that exhibited well–defined "river" patterns. Intergranular facets were rarely observed, but when they were found, it was mostly in the more heavily sensitized alloys.

Fatigue striations normal to the crack advance direction were clearly visible beyond ≈200 μm on the fracture surfaces for all material and environmental conditions. Striations were found on both the TG and IG facets of the samples tested in BWR conditions, or co-existing with the "river" patterns specific to the samples tested in the PWR environment. Evidence of extensive rubbing due to repeated contact between the two mating surfaces was also found.

The orientation of the cracks as they were initiated at the specimen surface was also a function of the test environment. For air tests, cracks were initiated obliquely, approaching 45°, with respect to the tensile axis. By contrast, for tests in either a BWR or PWR environment, crack initiation tended to be perpendicular to the tensile axis. In all environments, the overall orientation of the crack became perpendicular to the tensile axis as the crack grew beyond the initiation stage.

In air, the fatigue lives of Types 304 and 316 SS are comparable; those of Type 316NG are superior to those of Types 304 and 316 SS at high strain amplitudes. The fatigue lives of austenitic SSs in air are independent of temperature in the range from room temperature to 427°C. Also, variation in strain rate in the range of 0.4–0.008%/s has no effect on the fatigue lives of SSs at temperatures up to 400°C. The fatigue ε–N behavior of cast SSs is similar to that of wrought austenitic SSs.

Review of the available data shows that the fatigue lives of cast and wrought austenitic SSs are decreased in LWR environments. The decrease depends on strain rate, DO level in water, and temperature.

A minimum threshold strain is required for environmentally assisted decrease in the fatigue life of SSs, and this strain appears to be independent of material type (weld or base metal) and temperature in the range of 250–325°C. Environmental effects on fatigue life occur primarily during the tensile–loading cycle and at strain levels greater than the threshold value. Strain rate and temperature have a strong effect on fatigue life in LWR environments. Fatigue life decreases logarithmically with decreasing strain rate below 0.4%/s; the effect saturates at 0.0004%/s. Similarly, the fatigue ε–N data suggest a threshold temperature of 150°C; in the range of 150–325°C, the logarithm of life decreases linearly with temperature.

The fatigue lives of wrought and cast austenitic SSs are decreased significantly in low–DO (i.e., <0.01 ppm DO) water. In these environments, the composition or heat treatment of the steel has little or no effect on fatigue life. However, in high–DO water, the environmental effects on fatigue life are influenced by the composition and heat treatment of the steel. For a high–carbon heat of Type 304 SS, environmental effects were significant only for sensitized steel. For a low–carbon heat of Type 316NG SS, some effect of environment was observed even for mill–annealed steel in high–DO water, although the effect was smaller than that observed in low–DO water. Limited fatigue ε–N data indicate that the fatigue lives of cast SSs are approximately the same in low– and high–DO water and are comparable to those observed for wrought SSs in low–DO water.

Statistical models for the fatigue life of austenitic SSs as a function of material, loading, and environmental parameters have been developed. The functional form of the model and bounding values

of the important parameters are based on experimental observations and data trends. The models are recommended for predicted fatigue lives $\leq 10^6$ cycles. Consistent with previous work by Jaske and O'Donnell, the present results indicate that, even in air, the ASME mean curve for SSs is not consistent with the experimental data; it is nonconservative. Results that correspond to the 50th percentile of the statistical model are considered to be the best fit to the experimental data.

Two approaches are presented for incorporating the effects of LWR environments into ASME Section III fatigue evaluations**.** In the first approach, environmentally adjusted fatigue design curves are developed by adjusting the best–fit experimental curve for the effect of mean stress and by setting margins of 20 on cycles and 2 on strain to account for the uncertainties in life associated with material and loading conditions. These curves provide allowable cycles for fatigue crack initiation in LWR coolant environments. The second approach considers the effects of reactor coolant environments on fatigue life in terms of an environmental correction factor F_{en}, which is the ratio of fatigue life in air at room temperature to that in water under reactor operating conditions. To incorporate environmental effects into the ASME Code fatigue evaluations, a fatigue usage factor for a specific load set, based on the current Code design curves, is multiplied by the correction factor.

Acknowledgments

The authors thank T. M. Galvin, J. Tezak, and E. J. Listwan for their contributions to the experimental effort. This work is sponsored by the Office of Nuclear Regulatory Research, U.S. Nuclear Regulatory Commission, Job Code Y6388; Program Manager: W. H. Cullen, Jr.

1 Introduction

Cyclic loadings on a structural component occur because of changes in mechanical and thermal loadings as the system goes from one load set (e.g., pressure, temperature, moment, and force loading) to any other load set. For each load set, an individual fatigue usage factor is determined by the ratio of the number of cycles anticipated during the lifetime of the component to the allowable cycles. Figures I–9.1 through I–9.6 of Appendix I to Section III of the ASME Boiler and Pressure Vessel Code specify fatigue design curves that define the allowable number of cycles as a function of applied stress amplitude. The cumulative usage factor (CUF) is the sum of the individual usage factors, and the ASME Code Section III requires that the CUF at each location must not exceed 1.

The ASME Code fatigue design curves, given in Appendix I of Section III, are based on strain–controlled tests of small polished specimens at room temperature in air. The design curves have been developed from the best–fit curves to the experimental fatigue–strain–vs.–life (ε–N) data that are expressed in terms of the Langer equation[1] of the form

$$\varepsilon_a = A1(N)^{-n1} + A2, \tag{1}$$

where ε_a is the applied strain amplitude, N is the fatigue life, and A1, A2, and n1 are coefficients of the model. Equation 1 may be written in terms of stress amplitude S_a instead of ε_a, in which case stress amplitude is the product of ε_a and elastic modulus E, i.e., $S_a = E\,\varepsilon_a$. The fatigue design curves were obtained from the best–fit curves by first adjusting for the effects of mean stress on fatigue life and then reducing the fatigue life at each point on the adjusted curve by a factor of 2 on strain (or stress) or 20 on cycles, whichever is more conservative.

The factors of 2 and 20 are not safety margins but rather conversion factors that must be applied to the experimental data to obtain reasonable estimates of the lives of actual reactor components. Although the Section III criteria document[2] states that these factors were intended to cover such effects as environment, size effect, and scatter of data, Subsection NB–3121 of Section III of the Code explicitly notes that the data used to develop the fatigue design curves (Figs. I–9.1 through I–9.6 of Appendix I to Section III) did not include tests in the presence of corrosive environments that might accelerate fatigue failure. Article B–2131 in Appendix B to Section III states that the owner's design specifications should provide information about any reduction to fatigue design curves that has been necessitated by environmental conditions.

The existing fatigue ε–N data illustrate potentially significant effects of light water reactor (LWR) coolant environments on the fatigue resistance of carbon and low–alloy steels,[3–5] as well as of austenitic stainless steels (SSs).[4–7] Under certain environmental and loading conditions, fatigue lives of austenitic SSs can be a factor of 20 lower in water than in air.[6]

In LWR environments, the fatigue lives of austenitic SSs depend on applied strain amplitude, strain rate, temperature, and dissolved oxygen (DO) in water. A minimum threshold strain is required for environmentally assisted decrease in the fatigue life.[7] Environmental effects on life occur primarily during the tensile–loading cycle and at strain levels greater than the threshold value. Strain rate and temperature have a strong effect on fatigue life in LWR environments.[6,7] Fatigue life decreases logarithmically with decreasing strain rate below 0.4%/s; the effect saturates at 0.0004%/s. Similarly, the fatigue ε–N data suggest a threshold temperature of 150°C; in the range of 150–325°C, the logarithm of life decreases linearly with temperature. The effect of DO on fatigue life may depend on the composition

and heat treatment of the steel. Limited data indicate that, in high–DO water, the magnitude of environmental effects is influenced by material heat treatment.[7] In low–DO water, material heat treatment seems to have little or no effect on the fatigue life of austenitic SSs.

Two approaches have been proposed for incorporating the environmental effects into ASME Section III fatigue evaluations for primary pressure boundary components in operating nuclear power plants: (a) develop new fatigue design curves for LWR applications, or (b) use an environmental correction factor to account for the effects of the coolant environment. In the first approach, following the same procedures used to develop the current fatigue design curves of the ASME Code, environmentally adjusted fatigue design curves are developed from fits to experimental data obtained in LWR environments. Interim fatigue design curves that address environmental effects on the fatigue life of carbon and low–alloy steels and austenitic SSs were first proposed by Majumdar et al.[8] Fatigue design curves based on a more rigorous statistical analysis of experimental data were developed by Keisler et al.[9] These design curves have subsequently been updated on the basis of updated statistical models.[4,5]

The second approach, proposed by Higuchi and Iida,[10] considers the effects of reactor coolant environments on fatigue life in terms of an environmental correction factor F_{en}, which is the ratio of fatigue life in air at room temperature to that in water under reactor operating conditions. To incorporate environmental effects into fatigue evaluations, the fatigue usage factor for a specific load set, based on the current Code design curves, is multiplied by the environmental correction factor. Specific expressions for F_{en}, based on the Argonne National Laboratory (ANL) statistical models[4,5] and on the correlations proposed by the Ministry of International Trade and Industry (MITI) of Japan,[11] have been proposed.

This report presents experimental data on the effect of heat treatment on fatigue crack initiation in austenitic Type 304 SS in LWR coolant environments. A detailed metallographic examination of fatigue test specimens was performed to characterize the crack morphology and fracture morphology in austenitic SSs in air, and boiling water reactor (BWR) and pressurized water reactor (PWR) environments. The key material, loading, and environmental parameters and their effect on the fatigue life of these steels are also described. Statistical models are presented for estimating the fatigue ε–N curves for austenitic SSs as a function of material, loading, and environmental parameters. The two methods for incorporating the effects of LWR coolant environments into the ASME Code fatigue evaluations are presented.

2 Experimental

Fatigue tests have been conducted on two heats of Type 304 SS in the mill–annealed (MA) as well as MA plus additional heat treatment conditions. The chemical compositions of the heats are given in Table 1. Heat 10285 was heat treated at 600°C for 24 h whereas two heat treatments were used for Heat 30956, 0.67 h at 700°C and 24 h at 700°C. These heat treatments correspond to EPR (electrochemical potentiodynamic reactivation) values of ≈16 C/cm^2 for Heat 10285,[12] and ≈8 and 30 C/cm^2, respectively, for Heat 30956.[13]

Table 1. Composition (wt.%) of austenitic stainless steels for fatigue tests

Material	Source	C	P	S	Si	Cr	Ni	Mn	Mo
Type 304[a]	Supplier	0.060	0.019	0.007	0.48	18.99	8.00	1.54	0.44
Type 304[b]	Supplier	0.060	0.025	0.011	0.59	18.31	8.51	1.58	0.38

[a]76 x 25 mm bar stock, Heat 30956. Solution annealed at 1050°C for 0.5 h.
[b]25–mm–thick plate, Heat 10285. Solution annealed at 1050°C for 0.5 h.

The metallographic examination of the sensitized alloys was carried out on 10 x 10 x 10–mm specimens that were ground and polished with SiC paper by successively increasing the grade of the paper up to #4000, and subsequently finished with 1–μm diamond paste. Next, the samples were electrochemically etched in a solution of HNO_3 (10%) and distilled water at 8 V for ≈15 s. The examination of the microstructure was performed by scanning electron microscopy (SEM) in a JEOL JSM–6400 microscope.

Typical photomicrographs obtained from the sensitized alloys are shown in Fig. 1. Etching revealed a partially sensitized microstructure for the MA Heat 30956 that was heat treated for 0.67 h at 700°C. This is most evident in the higher–magnification photomicrograph (Fig. 1b) showing that sensitization occurred selectively, most likely at curved, high–energy boundaries. A somewhat more uniform degree of sensitization was observed in MA Heat 10285 (heat–treated for 24 h at 600°C), where almost all nontwin boundaries were sensitized. Stringers, also observed in this heat, most likely were parts of the microstructure before the sensitization treatment. Sensitization of Heat 30956 for 24 h at 700°C affected all of the boundaries, especially the curved, high–energy ones; also, it appears that some incoherent twin boundaries were also affected (Fig. 1f).

Smooth cylindrical specimens, with a 9.5–mm diameter and a 19–mm gauge length, were used for the fatigue tests (Fig. 2). The test specimens were machined from a composite bar fabricated by electron–beam welding of two 19.8–mm–diameter, 137–mm–long pieces of Type 304 SS bar stock on to each side of an 18.8–mm–diameter, 56–mm–long section of the test material, Fig. 3. The gauge section of the specimens was oriented along the rolling direction for the bar and plate stock. The gauge length of all specimens was given a 1–μm surface finish in the axial direction to prevent circumferential scratches that might act as sites for crack initiation.

Heat 30956, mill annealed plus heat treated 0.67 h at 700°C

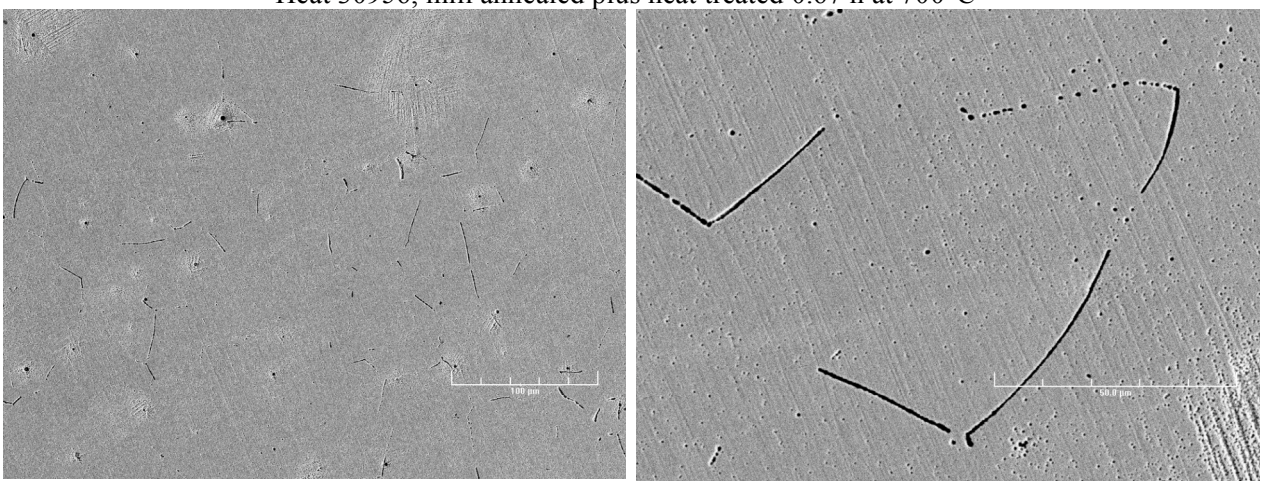

(a) (b)

Heat 10285, mill annealed plus heat treated 24 h at 600°C

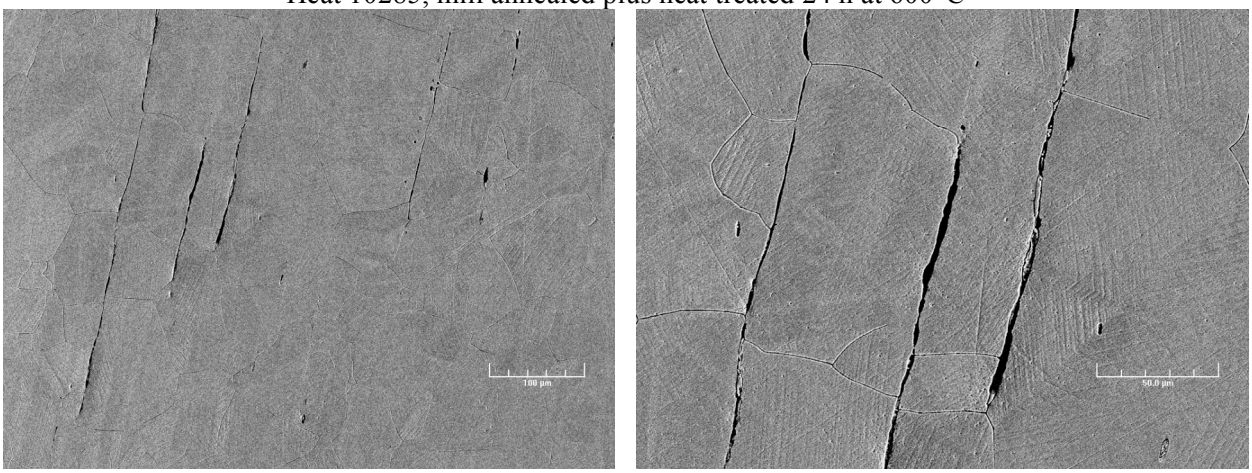

(c) (d)

Heat 30956, mill annealed plus heat treated 24 h at 700°C

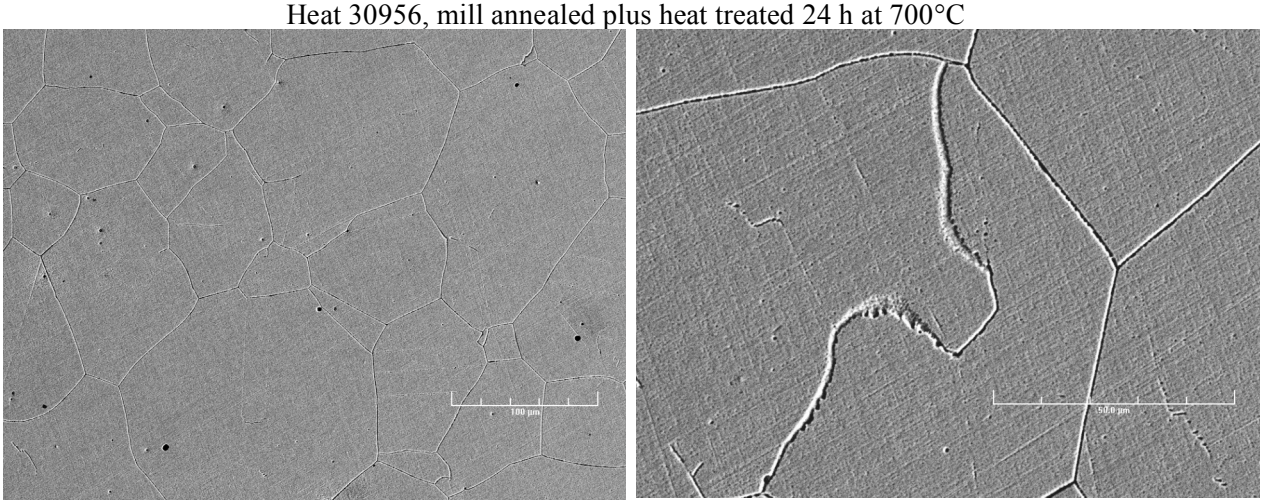

(e) (f)

Figure 1. Typical microstructures observed by SEM, showing degree of sensitization for alloys used in this study: (a), (c), (e), low magnification; (b), (d), (f), high magnification.

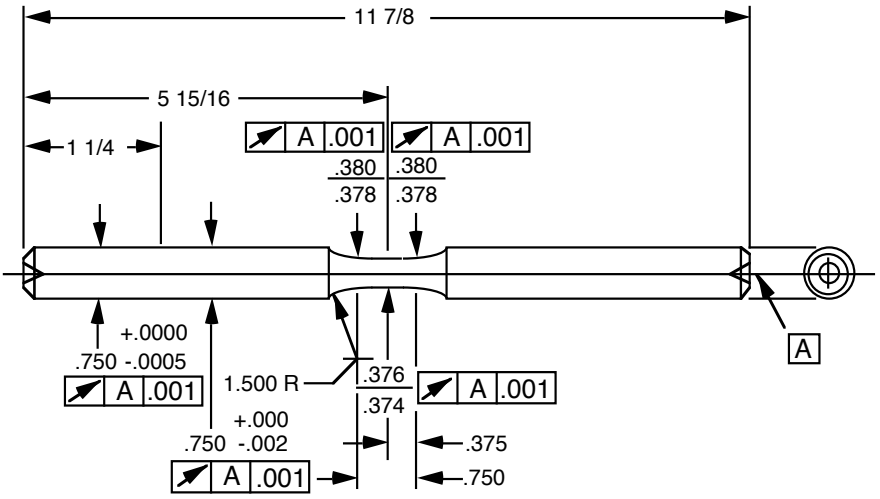

Figure 2. Configuration of fatigue test specimen (all dimensions in inches).

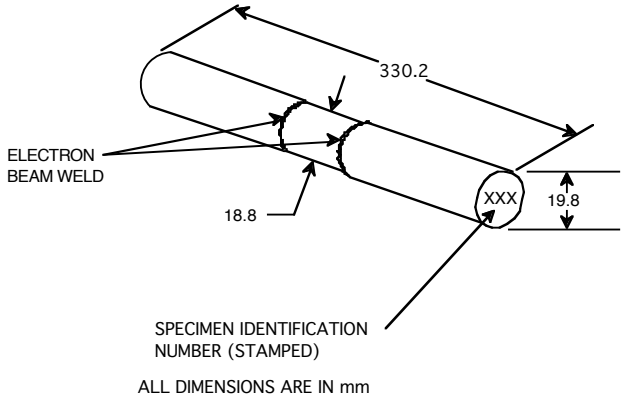

Figure 3. Schematic diagram of electron–beam–welded bar for machining A302–Gr B fatigue test specimens.

Tests in water were conducted in a 12–mL autoclave (Fig. 4) equipped with a recirculating water system that consisted of a 132–L closed feedwater storage tank, Pulsafeeder™ high–pressure pump, regenerative heat exchanger, autoclave preheater, test autoclave, electrochemical potential (ECP) cell, back-pressure regulator, ion exchange bed, 0.2–micron filter, and return line to the tank. Water was circulated at a rate of 10–15 mL/min. Water quality was maintained by circulating water in the feedwater tank through an ion exchange cleanup system. An Orbisphere meter and CHEMetrics™ ampules were used to measure the DO concentrations in the supply and effluent water. The redox and open–circuit corrosion potentials, respectively, were monitored at the autoclave outlet by measuring the ECPs of platinum and an electrode of the test material, against a 0.1–M KCl/AgCl/Ag external (cold) reference electrode. The measured ECPs, $E_{(meas)}$ (mV), were converted to the standard hydrogen electrode (SHE) scale, $E_{(SHE)}$ (mV), by solving the polynomial expression[14]

$$E_{(SHE)} = E_{(meas)} + 286.637 - 1.0032(\Delta T) + 1.7447 \times 10^{-4}(\Delta T)^2 - 3.03004 \times 10^{-6}(\Delta T)^3, \quad (2)$$

where ΔT(°C) is the temperature difference of the salt bridge in a 0.1–M KCl/AgCl/Ag external reference electrode (i.e., the test temperature minus ambient temperature). A description of the test facility has been presented earlier.[6,15]

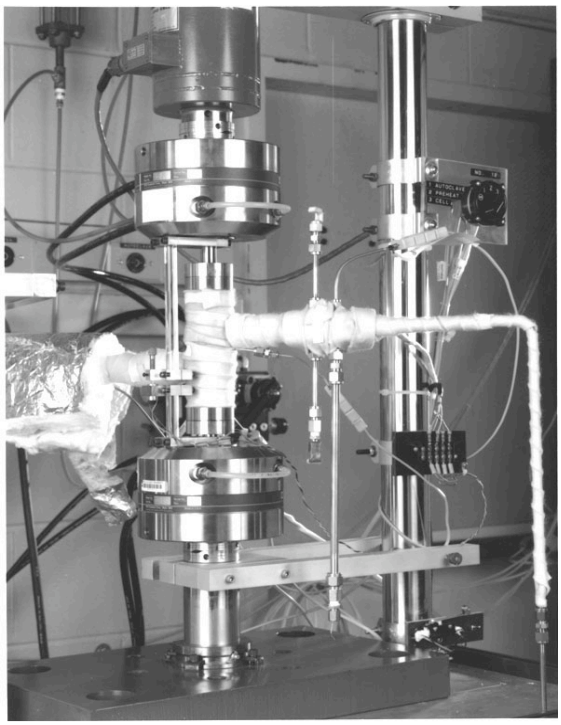

Figure 4.
Autoclave system for fatigue tests in water.

Boiling water reactor conditions were established by bubbling N_2 that contained 1–2% O_2 through deionized water in the supply tank. The deionized water was prepared by passing purified water through a set of filters that comprise a carbon filter, an Organex–Q filter, two ion exchangers, and a 0.2–mm capsule filter. Water samples were taken periodically to measure pH, resistivity, and DO concentration. When the desired concentration of DO was attained, the N_2/O_2 gas mixture in the supply tank was maintained at a 20–kPa overpressure. After an initial transition period, during which an oxide film developed on the fatigue specimen, the DO level and the ECP in the effluent water remained constant. Test conditions are described in terms of the DO in effluent water.

Simulated PWR water was obtained by dissolving boric acid and lithium hydroxide in 20 L of deionized water before adding the solution to the supply tank. The DO in the deionized water was reduced to <10 ppb by sparging it with either pure N_2 or a mixture of N_2 plus 5% H_2. A vacuum was drawn on the tank cover gas to speed deoxygenation. After the DO was reduced to the desired level, a 34–kPa overpressure of H_2 was maintained to provide ≈2 ppm dissolved H_2 (or ≈23 cc^3/kg) in the feedwater.

All tests were conducted at 289°C, with fully reversed axial loading (i.e., R = –1) and a sawtooth waveform. During the tests in water, performed under stroke control, the specimen strain was controlled between two locations outside the autoclave. Companion tests in air were performed under strain control with an axial extensometer. During the test, the stroke at the location used to control the water tests was recorded. Information from the air tests was used to determine the stroke required to maintain constant strain in the specimen gauge. To account for cyclic hardening of the material, the stroke that was needed to maintain constant strain was gradually increased during the test, based on the stroke measurements from the companion strain–controlled tests. The fatigue life N_{25} is defined as the number of cycles for tensile stress to decrease 25% from its peak or steady–state value.

Following testing, ≈10–mm–long sections that contained the fracture surface were cut from the gauge length. These were further stripped of oxides by boiling in a 20 wt.% NaOH and 3 wt.% $KMnO_4$ solution, followed by boiling in a 20 wt.% $(NH_4)_2C_6H_6O_7$ solution. The samples were examined by SEM. Special attention has been paid to crack morphology at the sites of initiation on the fracture surface, and the occurrence of striations. Also, lateral surfaces were inspected to determine the morphology of lateral cracks.

3 Results – Effect of Heat Treatment on Fatigue Life

3.1 Fatigue ε–N Behavior

Several fatigue tests have been completed on two heats of Type 304 SS under various heat–treatment conditions, and in air and simulated BWR and PWR environments at 289°C. The results from these tests and data obtained earlier on MA Heat 30956 are given in Table 2.

Table 2. Fatigue test results for Type 304 stainless steel in air and simulated BWR and PWR environments at 289°C

Test No.	Spec. No.	Environment[a]	Dis. Oxygen[b] (ppb)	pH at RT[c]	Conductivity[b] (μS/cm)	ECP Pt[b] mV (SHE)	ECP SS[b] mV (SHE)	Ten. Rate (%/s)	Comp. Rate (%/s)	Stress Amp. (MPa)	Strain Amp. (%)	Life N_{25} (Cycles)
Heat 30956 MA												
1805	309-03	Air	–	–	–	–	–	4.0E-3	4.0E-1	234.0	0.38	14,410
1853	309-22	BWR	880	6.0	0.06	248	155	4.0E-3	4.0E-1	233.3	0.38	12,300
1856	309-24	BWR	870	6.2	0.07	272	163	4.0E-3	4.0E-1	236.8	0.38	10,450
1808	309-06	PWR	4	6.4	18.87	-693	-690	4.0E-3	4.0E-1	234.2	0.39	2,850
1821	309-09	PWR	2	6.5	22.22	-700	-697	4.0E-3	4.0E-1	237.2	0.38	2,420
1859	309-28	PWR	2	6.5	18.69	-699	-696	4.0E-3	4.0E-1	235.9	0.38	2,420
Heat 30956 MA plus 0.67 h at 700°C												
1893	309-43	Air	–	–	–	–	–	4.0E-3	4.0E-1	236.9	0.38	17,000
1894	309-44	BWR	800	6.7	0.07	263	158	4.0E-3	4.0E-1	239.1	0.38	3,920
1899	309-46	BWR	800	6.2	0.06	285	126	4.0E-3	4.0E-1	241.4	0.38	3,740
1898	309-45	PWR	6	6.3	17.24	-677	-467	4.0E-3	4.0E-1	241.2	0.38	2,530
Heat 30956 MA plus 24 h at 700°C												
1891	309-47	Air	–	–	–	–	–	4.0E-3	4.0E-1	235.8	0.38	16,680
1892	309-48	BWR	860	–	0.06	257	119	4.0E-3	4.0E-1	237.3	0.39	2,790
1897	309-50	PWR	6	6.3	16.67	-629	-543	4.0E-3	4.0E-1	234.1	0.39	2,380
Heat 10285 MA plus 24 h at 600°C												
1895	102-07	Air	–	–	–	–	–	4.0E-3	4.0E-1	222.4	0.38	19,300
1896	102-09	BWR	800	–	0.1	265	206	4.0E-3	4.0E-1	222.2	0.39	1,665
1900	102-08	PWR	7	6.2	16.95	-522	-527	4.0E-3	4.0E-1	228.0	0.37	2,840

[a]PWR = simulated PWR water with 2 ppm Li, 1000 ppm B, and ≈2 ppm dissolved H_2 (or ≈23 cc/kg) in the feedwater; BWR = high-purity deionized water.
[b]Measured in effluent.
[c]RT = room temperature.

The effect of heat treatment on the fatigue life of Type 304 SS in air, BWR, and PWR environments is shown in Fig. 5. Fatigue life is plotted as a function of the EPR value for the various material conditions. The results indicate that heat treatment has little or no effect on the fatigue life of Type 304 SS in air and PWR environments. In a BWR environment, fatigue life is lower for the sensitized SSs. The decrease in life seems to increase with increasing EPR value.

The cyclic stress response of the various materials in air, BWR, and PWR environments at 289°C is shown in Fig. 6. As expected, the cyclic strain–hardening behavior of Type 304 SS under various heat treatment conditions is identical, only the fatigue life varies in the environments.

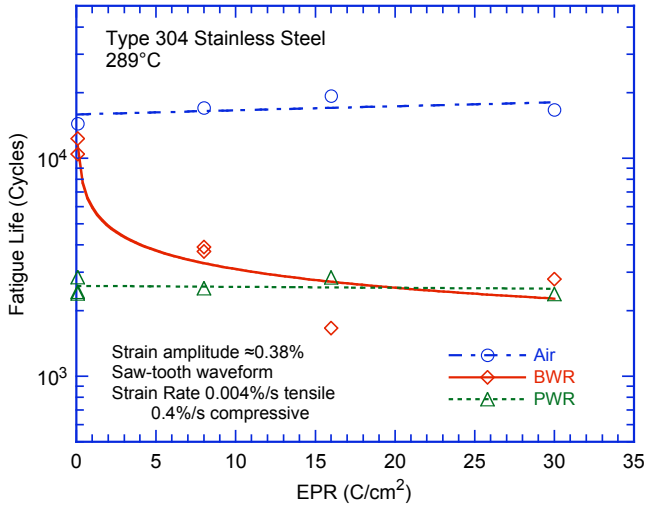

Figure 5.
The effect of material heat treatment on fatigue life of Type 304 stainless steel in air, BWR, and PWR environments at 289°C, ≈0.38% strain amplitude, sawtooth waveform, and 0.004%/s tensile strain rate.

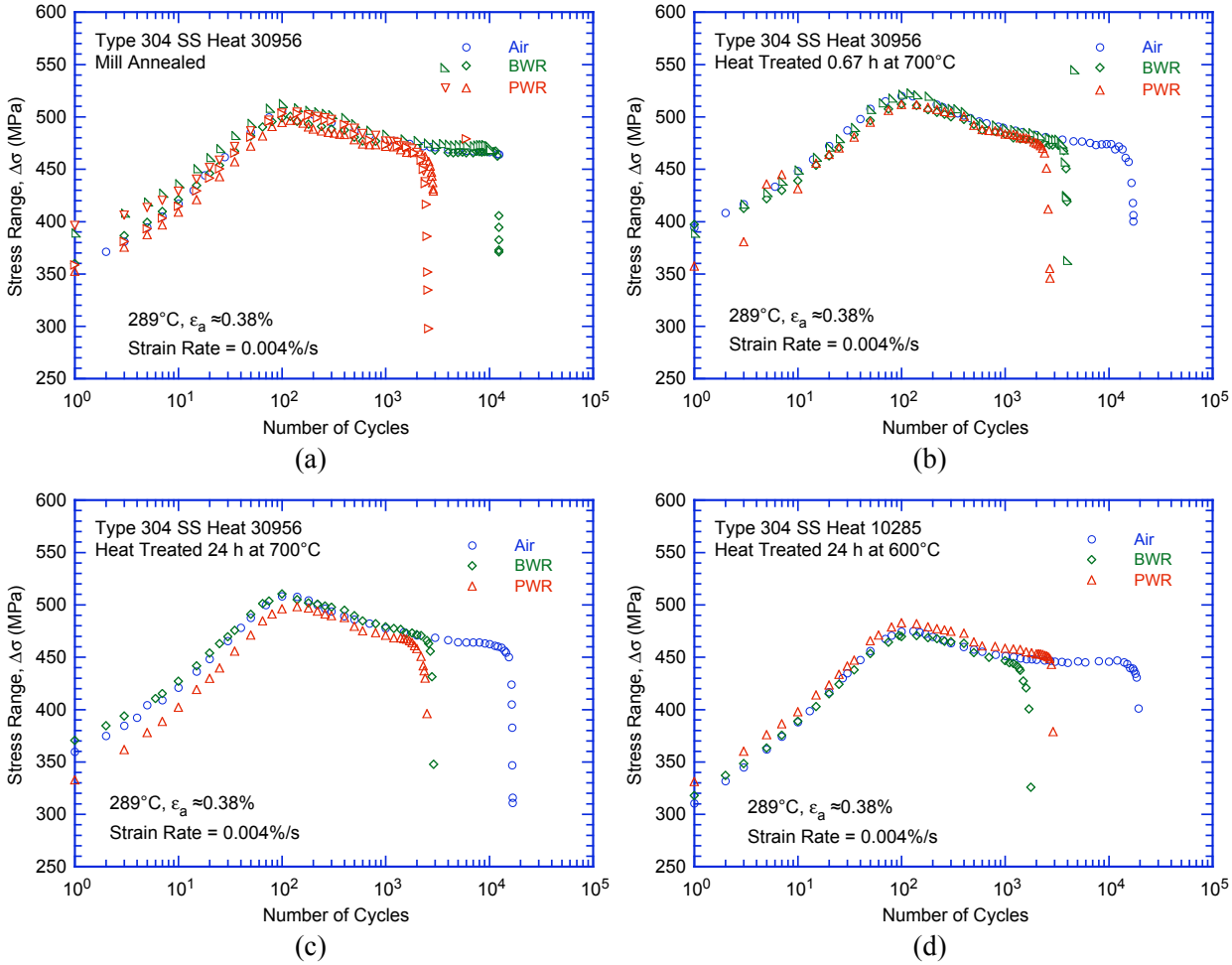

Figure 6. Cyclic stress response of Heat 30956, (a) MA, (b) MA + 0.67 h at 700°C, and (c) MA + 24 h at 700°C; and Heat 10285, (d) MA + 24 h at 600°C, in air, BWR, and PWR environments at 289°C.

3.2 Fatigue Crack and Fracture Surface Morphology

A detailed metallographic evaluation of the fatigue test specimens was performed to characterize the crack and fracture morphology of the various heats under various heat treatment conditions. Figure 7 shows low– and high–magnification crack initiation sites on the fracture surfaces of the sensitized Type 304 SS tested in air. It can be observed that, apparently irrespective of the degree of sensitization, the fracture mode for crack initiation (i.e., crack lengths up to ≈200 μm) and crack propagation (i.e., crack lengths >200 μm) is transgranular (TG), most likely along crystallographic planes, leaving behind relatively smooth facets. With increasing degree of sensitization, cleavage–like or stepped TG fracture (e.g., Figs. 7c and d), and occasionally ridge structures on the smooth surfaces (e.g., Figs. 7e and f) were observed.

An effect of a simulated normal–water chemistry BWR environment, Fig. 8, was to cause intergranular (IG) crack initiation, implying a weakening of the grain boundaries. In the BWR environment, the initial crack appeared IG under all heat–treated conditions. Photomicrographs of the fracture surface of the more heavily sensitized steel, e.g., Heat 30956 MA + 24 h at 700°C (Figs. 8g and h) and especially Heat 10285 MA + 24 h at 600°C (Figs. 8e and f), are good examples of smooth IG fracture. Furthermore, by comparing the four material conditions, it appears that the extent of IG fracture increases with the degree of sensitization, at least through the MA + 24 h at 600°C condition, whereas MA + 24 h at 700°C appears to have a somewhat more mixed IG and TG morphology. Also, one effect of the BWR environment (Figs. 8a–h) was to cause IG crack initiation, implying a weakening of the grain boundaries. Nevertheless, for all four conditions tested, initial IG mode transformed within <200 μm into a TG mode with cleavage–like features. By contrast, for all samples of Type 304 SS tested in PWR environments (Fig. 9), cracks initiated and propagated in a TG mode irrespective of the degree of sensitization. Prominent features of all fracture surfaces are highly angular, cleavage–like fracture facets that exhibit well–defined "river" patterns. Intergranular facets were rarely observed, mostly in the more heavily sensitized alloys. These observations suggest brittle behavior throughout the testing period.

Fatigue striations normal to the crack advance direction were clearly visible beyond ≈200 μm on the fracture surfaces of all materials under all environmental conditions, as documented in Figs. 10–13. For example, for the MA Heat 30956 samples tested in BWR water (Fig. 10), striations were easily discernible on the facets irrespective of the steps, cleavage–like features, or river patterns. Similar striations were also observed on the fracture surface of MA Heat 30956 heat–treated 0.67 h at 700°C irrespective of the testing environment (Fig. 11). Striations were found on both the TG and IG facets of the samples tested under BWR conditions, or co-existing with the "river" patterns specific to the samples tested in the PWR environment. Evidence of extensive rubbing due to repeated contact between the two mating surfaces (Figs. 11a and b) was also found.

Figure 12 shows fatigue striations observed on the fracture surface of MA Heat 10285 heat–treated 24 h at 600°C. In spite of the wide coverage with rubbing and fretting marks, striations are clearly observed on some facets. Figures 12e and f show striations on one IG facet in a sample tested in PWR conditions. The fracture surfaces of MA Heat 30956 heat–treated 24 h at 700°C are presented in Fig. 13. Low– and high–magnification photomicrographs are presented of fatigue striations on faceted, stepped TG, and cleavage–like fracture surfaces.

Air Environment

Heat 30956 mill annealed plus heat treated 0.67 h at 700°C

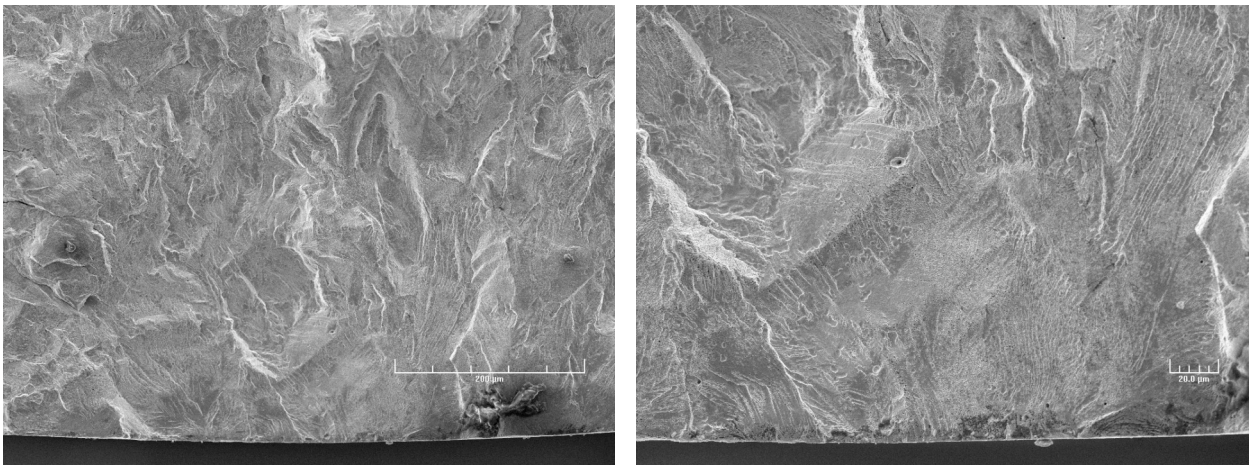

(a) (b)

Heat 10285 mill annealed plus heat treated 24 h at 600°C

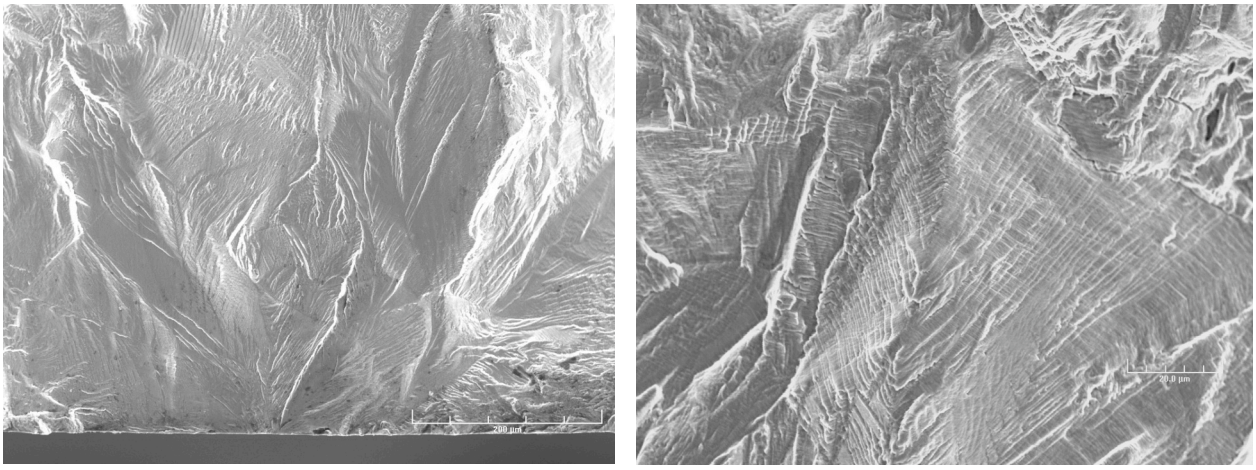

(c) (d)

Heat 30956 mill annealed plus heat treated 24 h at 700°C

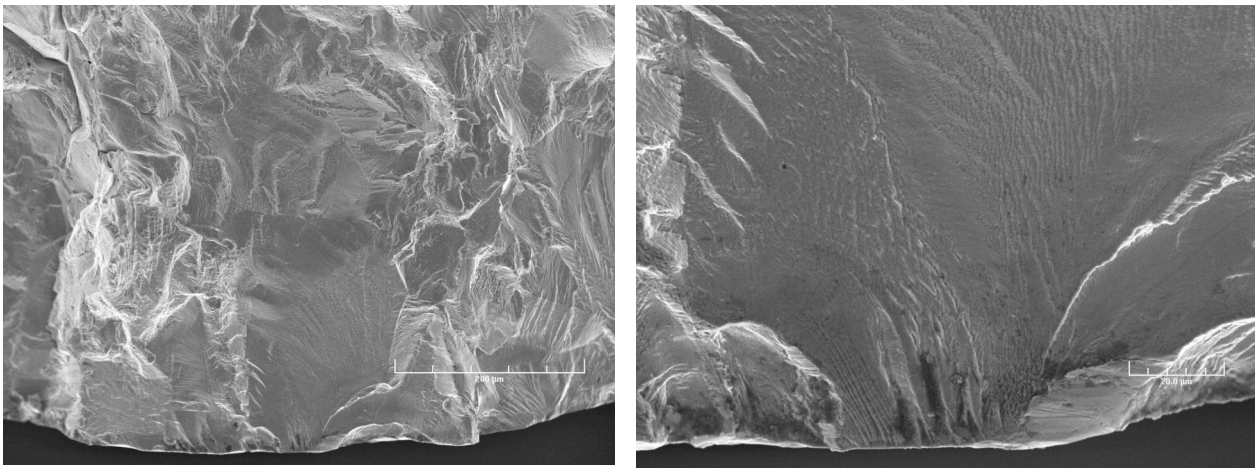

(e) (f)

Figure 7. Photomicrographs showing sites of crack initiation on fracture surfaces of Type 304 SS specimens tested in air: (a), (c), (e), low magnification; (b), (d), (f), high magnification.

Simulated BWR Environment

Heat 30956 mill annealed

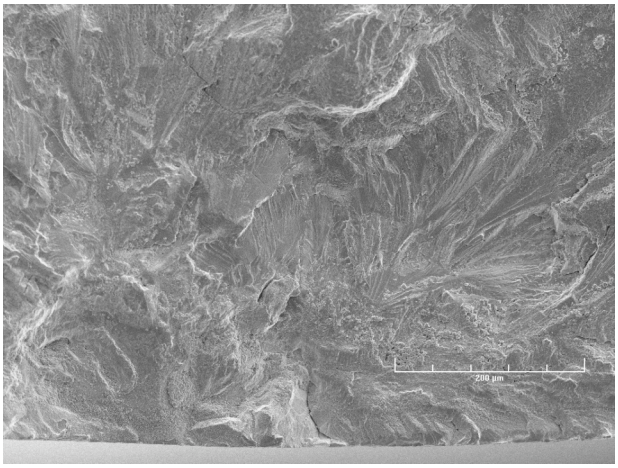

(a)

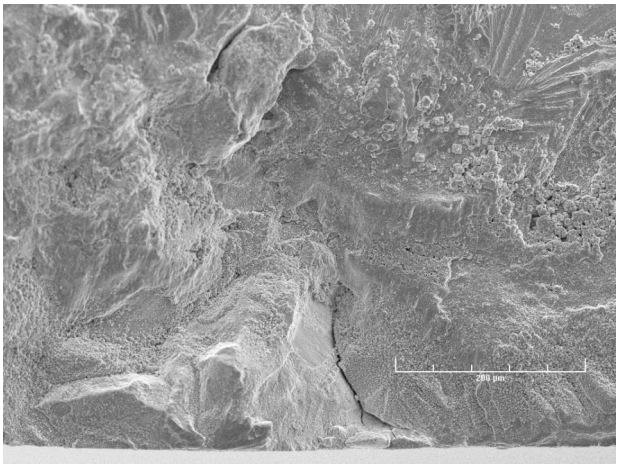

(b)

Heat 30956 mill annealed plus heat treated 0.67 h at 700°C

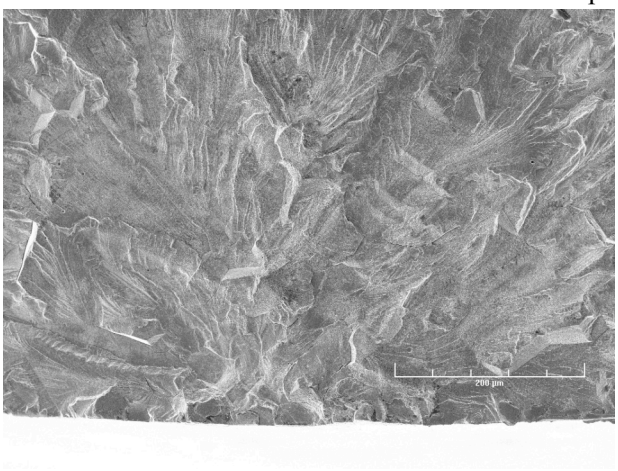

(c)

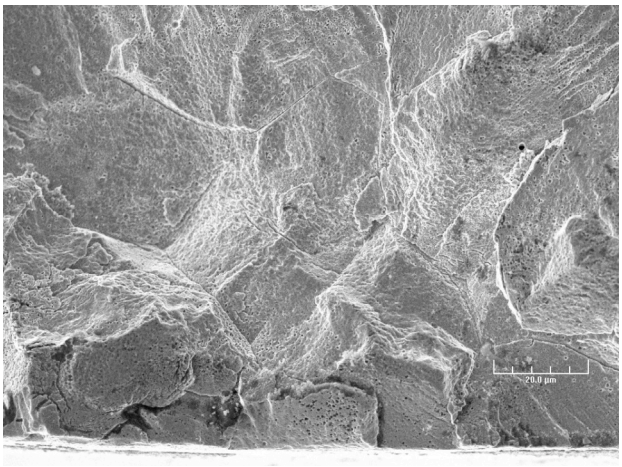

(d)

Heat 10285 mill annealed plus heat treated 24 h at 600°C

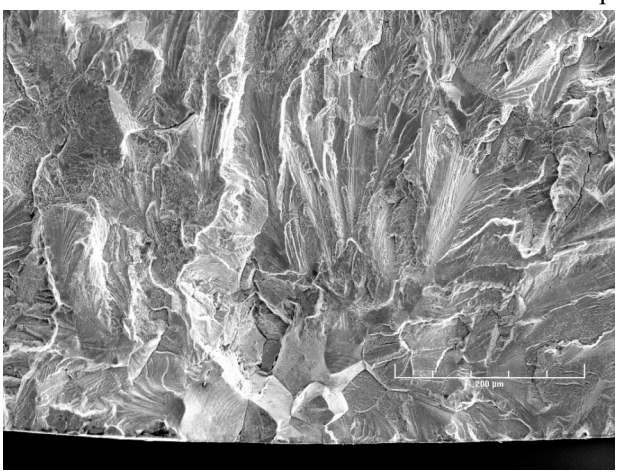

(e)

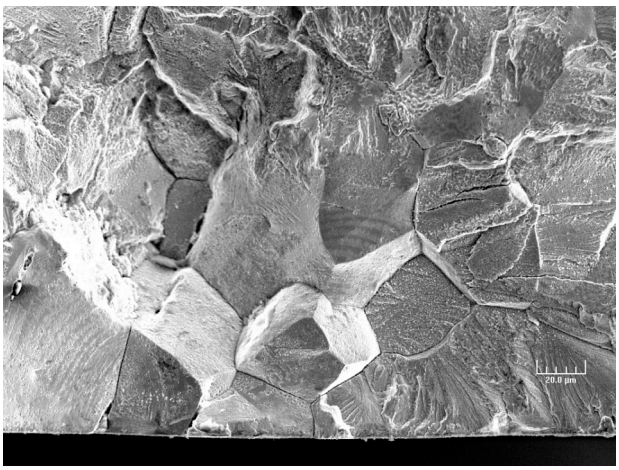

(f)

Heat 30956 mill annealed plus heat treated 24 h at 700°C

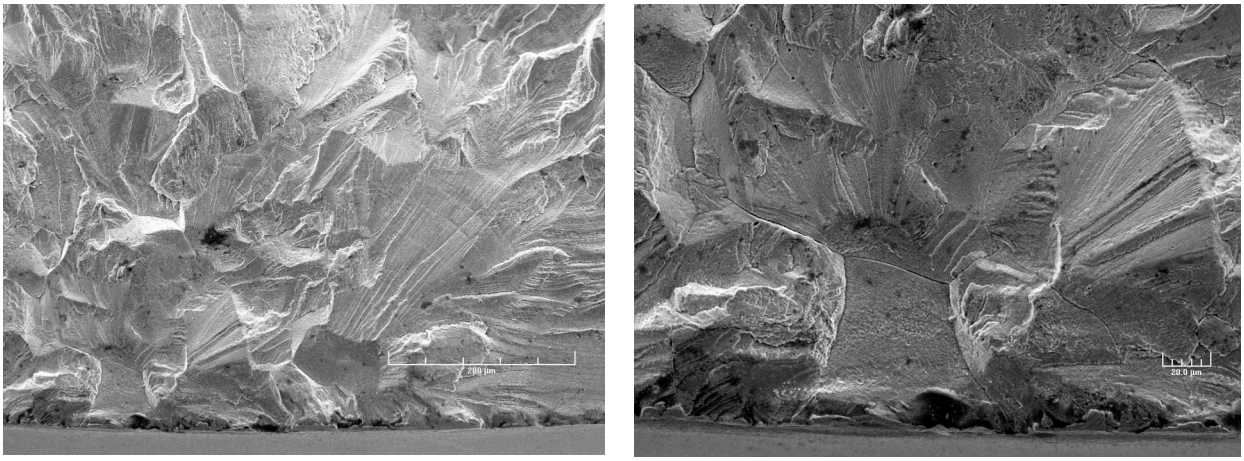

(g) (h)

Figure 8. Photomicrographs showing sites of crack initiation on fracture surfaces of Type 304 SS specimens tested in simulated BWR environment: (a), (c), (e), (g) low magnification; (b), (d), (f), (h) high magnification.

Simulated PWR Environment

Heat 30956 mill annealed

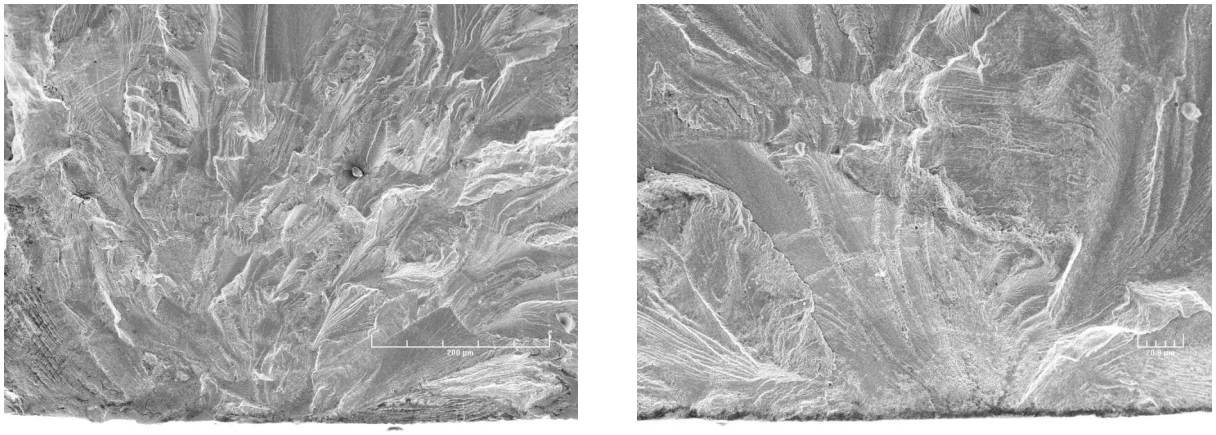

(a) (b)

Heat 30956 mill annealed plus 0.67 h at 700°C

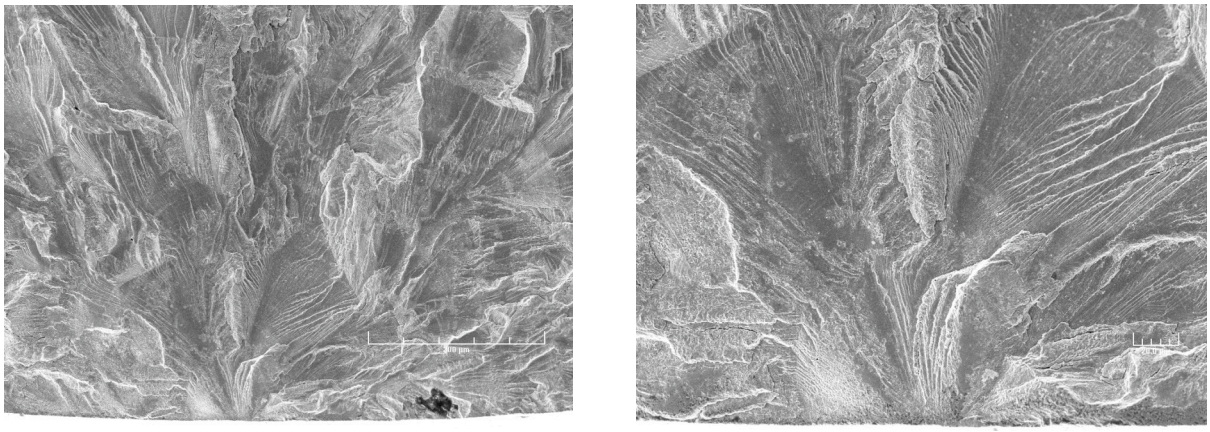

(c) (d)

Heat 10285 mill annealed plus 24 h at 600°C

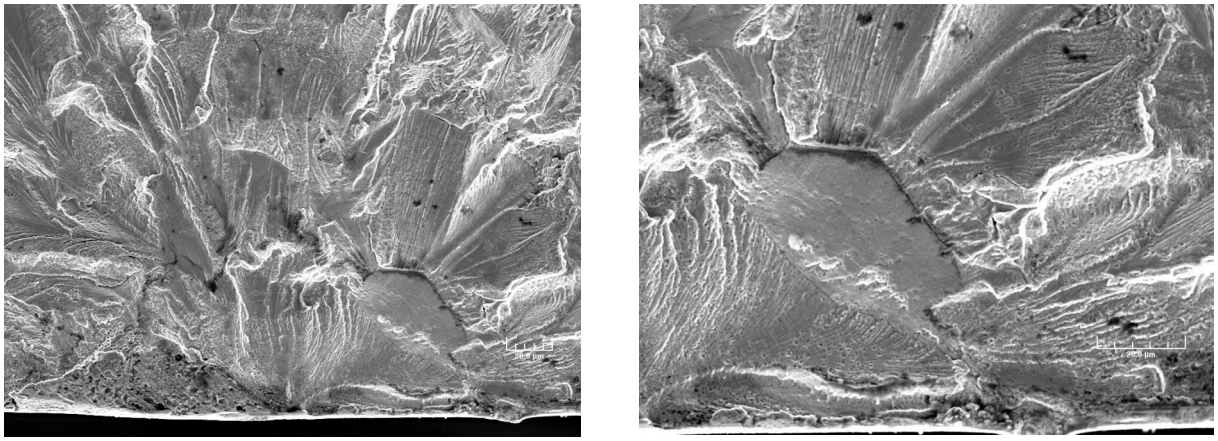

(e) (f)

Heat 30956 mill annealed plus 24 h at 700°C

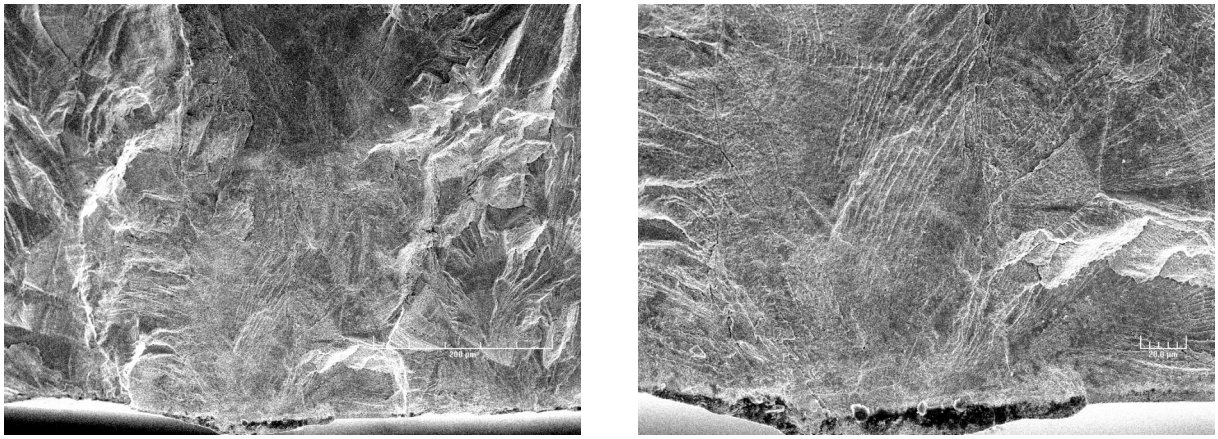

(g) (h)

Figure 9. Photomicrographs showing the sites of crack initiation on the fracture surfaces of Type 304 SS specimen tested in simulated PWR environment: (a), (c), (e), (g) low magnification; (b), (d), (f), (h) high magnification.

Simulated BWR environment

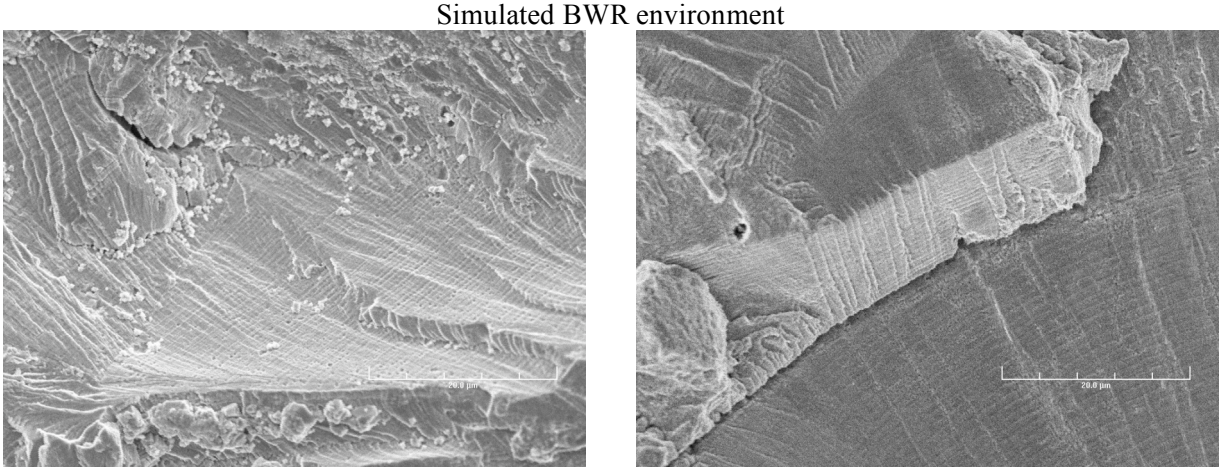

(a) (b)

Figure 10. (a) Low– and (b) high–magnification photomicrographs showing striations at select locations on fracture surfaces of MA specimen of Heat 30956 in simulated BWR environment.

Heat 30956 mill annealed plus 0.67 h at 700°C

Air Environment

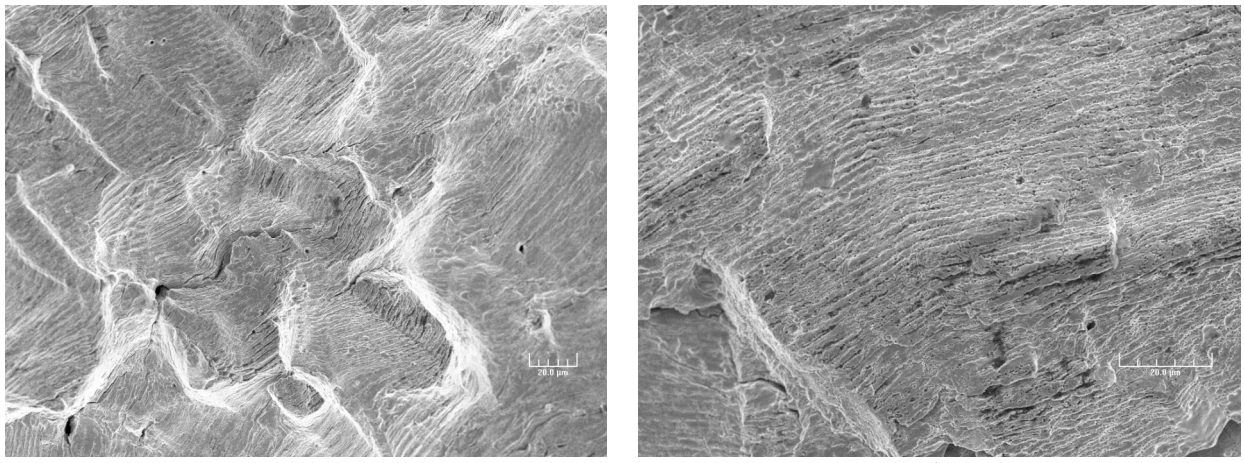

(a) (b)

Simulated BWR Environment

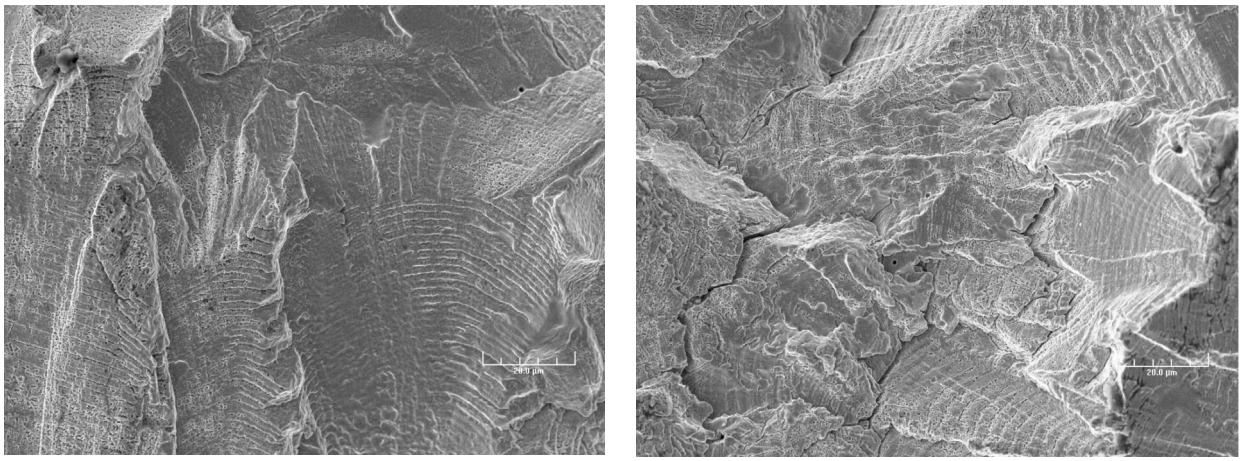

(c) (d)

Simulated PWR Environment

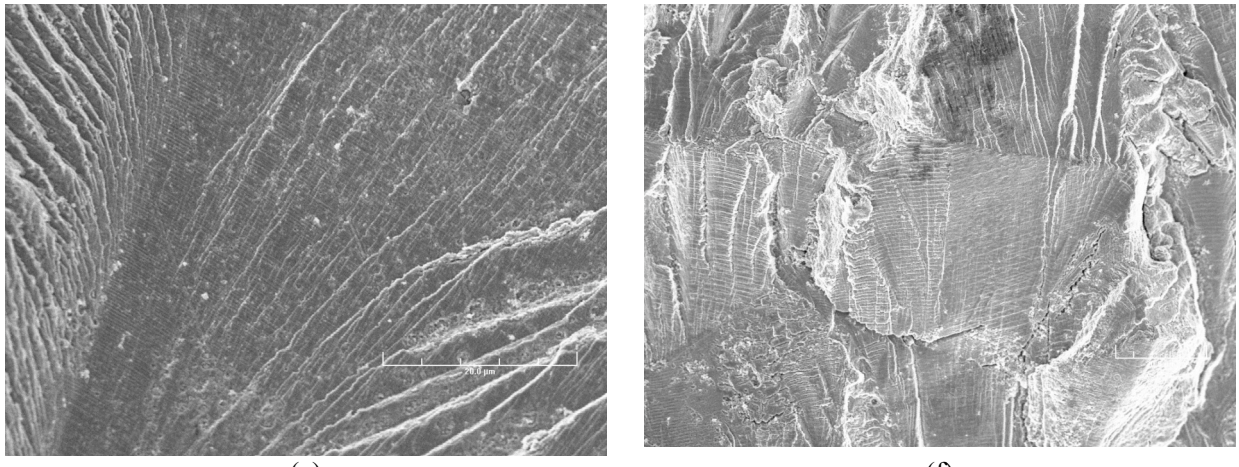

(e) (f)

Figure 11. Low– (a), (c), (e) and high–magnification (b), (d), (f) photomicrographs showing striations at select locations on fracture surfaces of MA specimens of Heat 30956 heat–treated for 0.67 h at 700°C in air, BWR, and PWR environments.

Heat 10285 mill annealed plus 24 h at 600° C

Air Environment

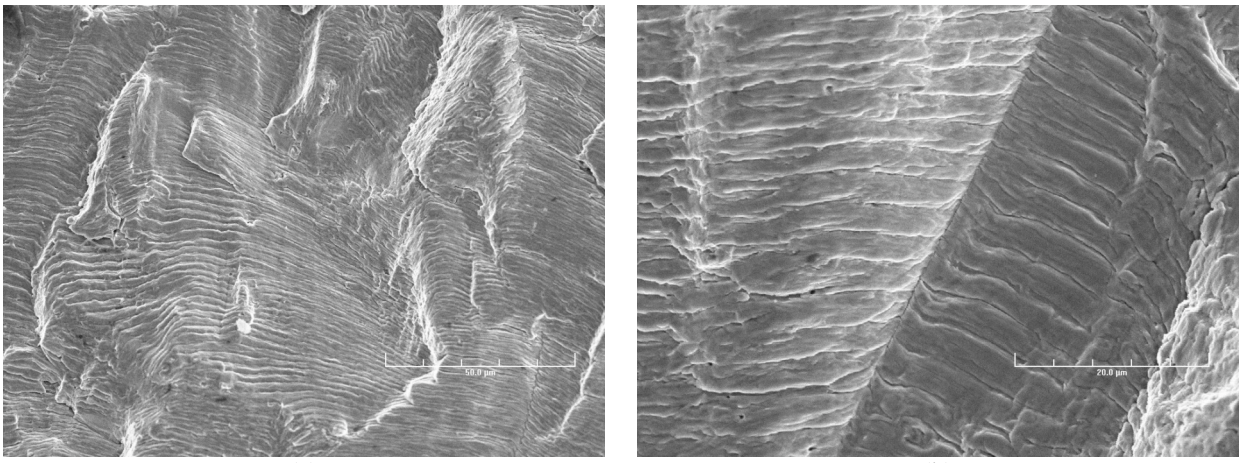

(a) (b)

Simulated BWR Environment

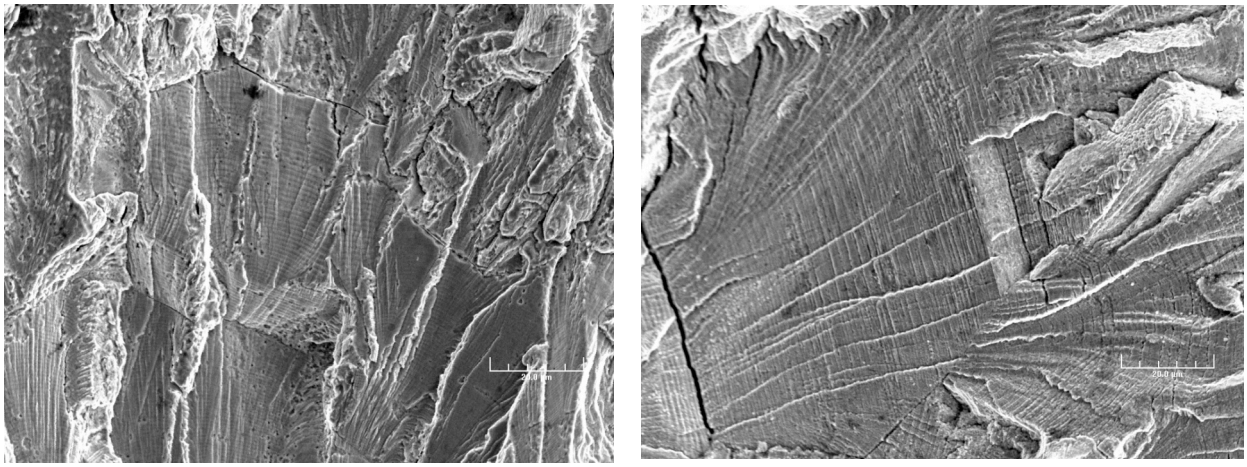

(c) (d)

Simulated PWR Environment

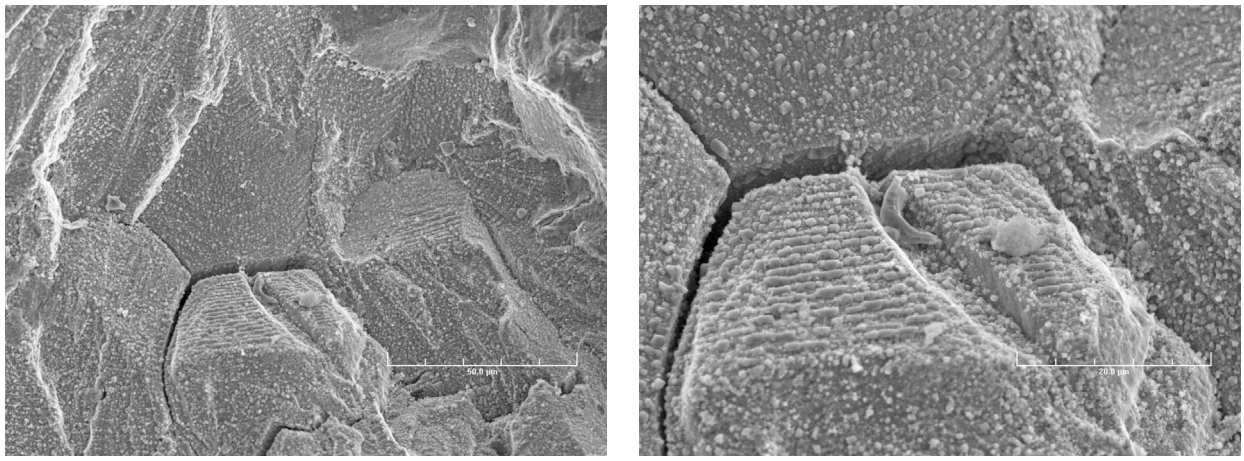

(e) (f)

Figure 12. Low– (a), (c), (e) and high–magnification (b), (d), (f) photomicrographs showing striations at select locations on fracture surfaces of MA specimens of Heat 10285 heat–treated for 24 h at 600°C in air, BWR, and PWR environments.

Heat 30956 mill annealed plus 24 h at 700°C

Air Environment

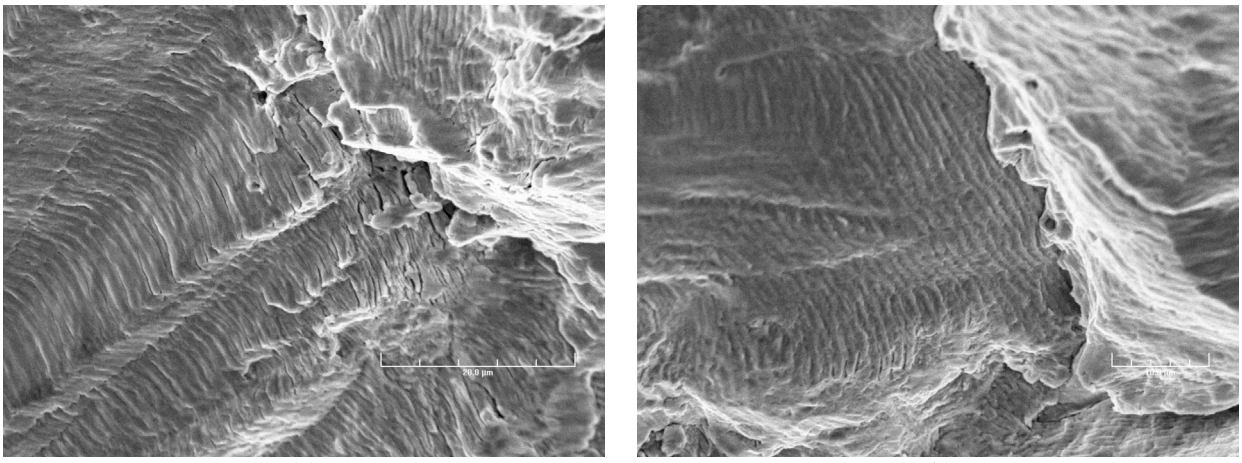

(a) (b)

Simulated BWR Environment

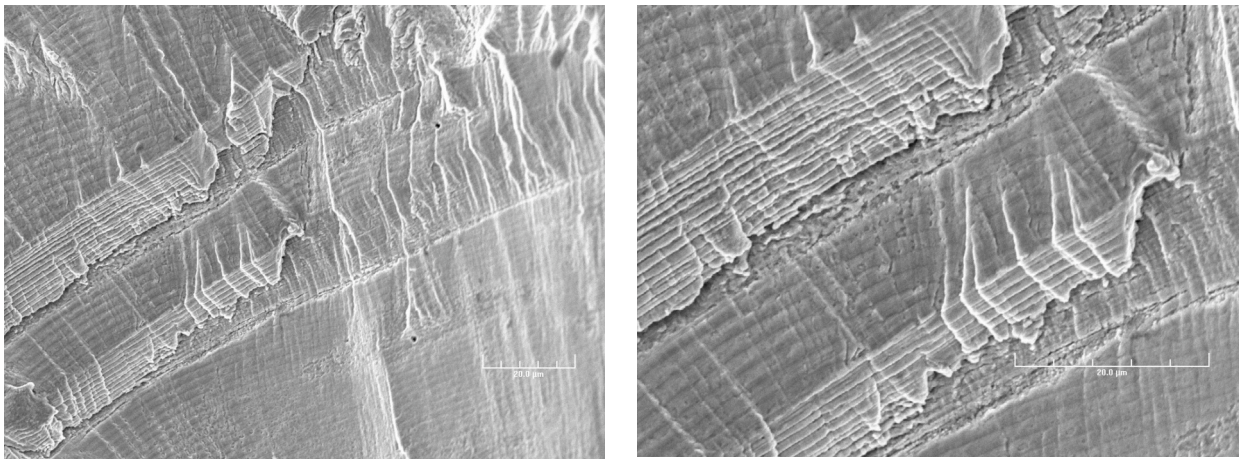

(c) (d)

Simulated PWR Environment

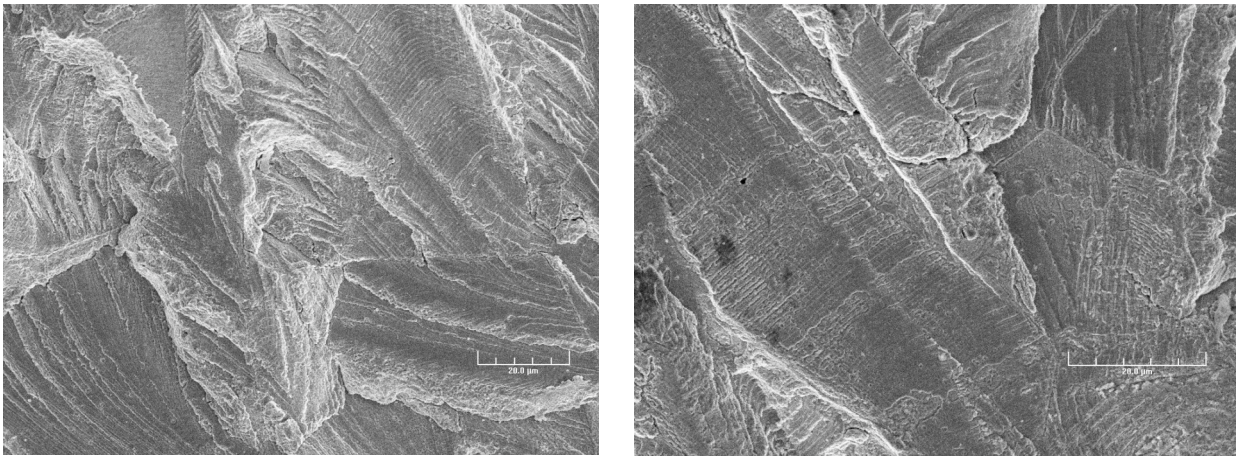

(e) (f)

Figure 13. Low– (a), (c), (e) and high–magnification (b), (d), (f) photomicrographs showing striations at select locations on fracture surfaces of MA specimens of Heat 30956 heat–treated for 24 h at 700°C in air, BWR, and PWR environments.

Photomicrographs of the crack morphology of Type 304 SS under all test and environmental conditions are presented in Fig. 14. In all cases, the tensile axis is vertical, parallel to the plane of each picture. In general, for air tests the cracks are more likely to be oblique, approaching 45° with respect to the tensile axis. By contrast, the cracks that form in either BWR or PWR environments tended to be perpendicular to the tensile axis.

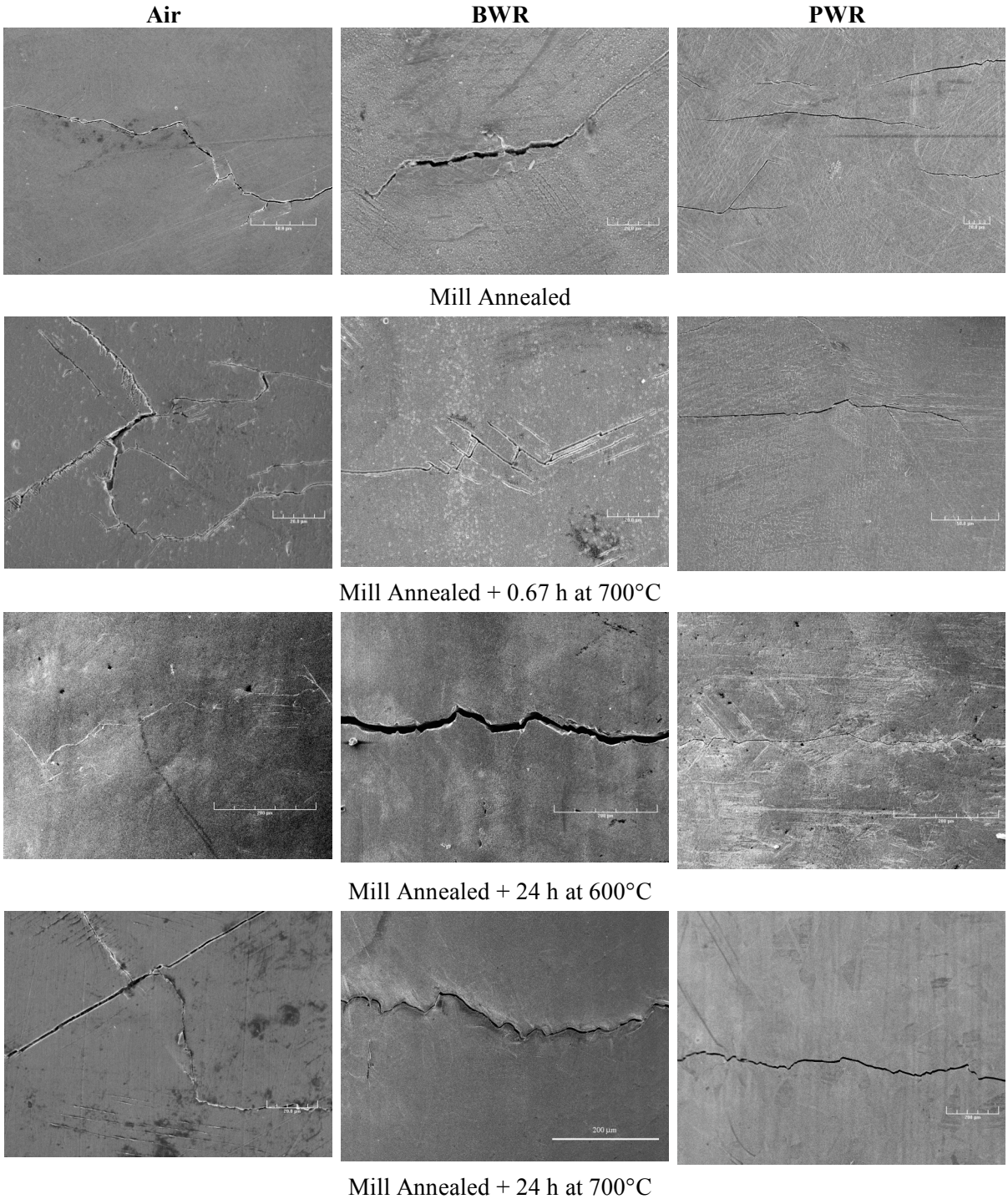

Figure 14. Photomicrographs of the crack morphology of Type 304 SS under all test and environmental conditions.

The results of the metallographic evaluations of the fatigue test specimens may be summarized as follows. In air, cracking was initiated as TG, oblique with respect to the tensile axis. In BWR environments, cracking was initiated as IG, normal to the tensile axis. By contrast, in PWR environments cracking was initiated as TG, but still normal to the tensile axis. Cracking propagated as TG irrespective of the environment.

The crack and fracture morphology in Type 316NG SS specimens (Heat D432804) from earlier tests was also evaluated for comparison. Figure 15 shows, at low and high magnification, crack initiation sites on the fracture surfaces of Type 316NG specimens tested in air. Note that the cracks were initiated and propagated in TG mode, most likely along crystallographic planes, leaving behind highly angular, cleavage–like or stepped surface features. Figures 15c and d show striations on some highly angular facets.

In a high–DO BWR environment, Fig. 16a–c, cracking was also initiated and propagated in TG mode, with riverlike patterns on the facets. Within 200 μm of the initiation site, fatigue striations were observed on some facets (Figs. 16b and c). Similarly, for specimens tested in a low–DO PWR environment (Fig. 16d), crack initiation and crack propagation are TG, with cleavage–like fracture facets

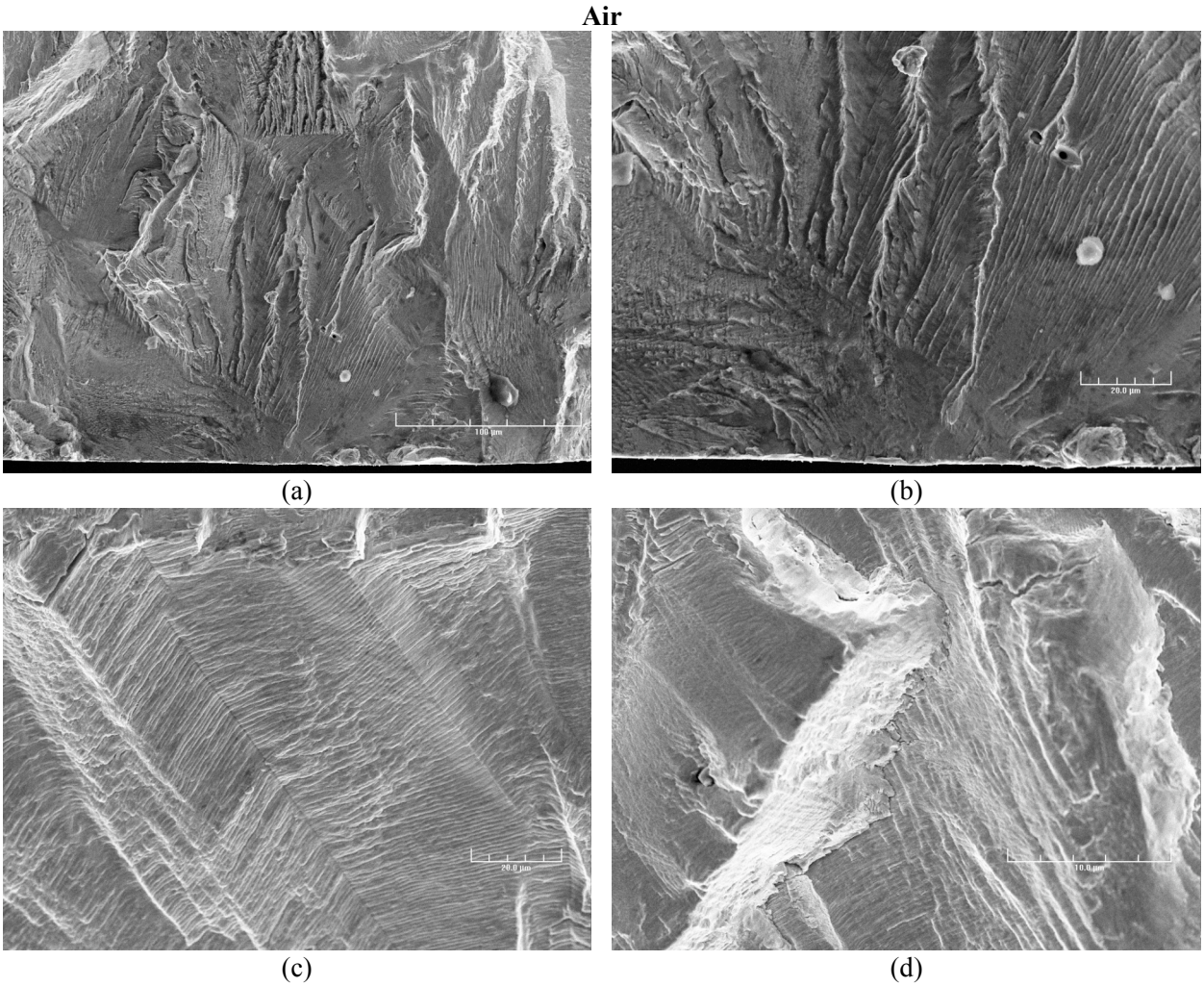

Figure 15. Photomicrographs showing crack initiation site at (a) low and (b) high magnification, and (c) and (d) striations at select locations in Type 316NG SS tested in air.

that exhibit river patterns. The higher magnification photomicrographs (at a location also seen in Fig. 16d) show fatigue striations within 200 μm of the initiation site. Evidence of rubbing due to repeated contact between the two mating surfaces can also be observed in Fig. 16f.

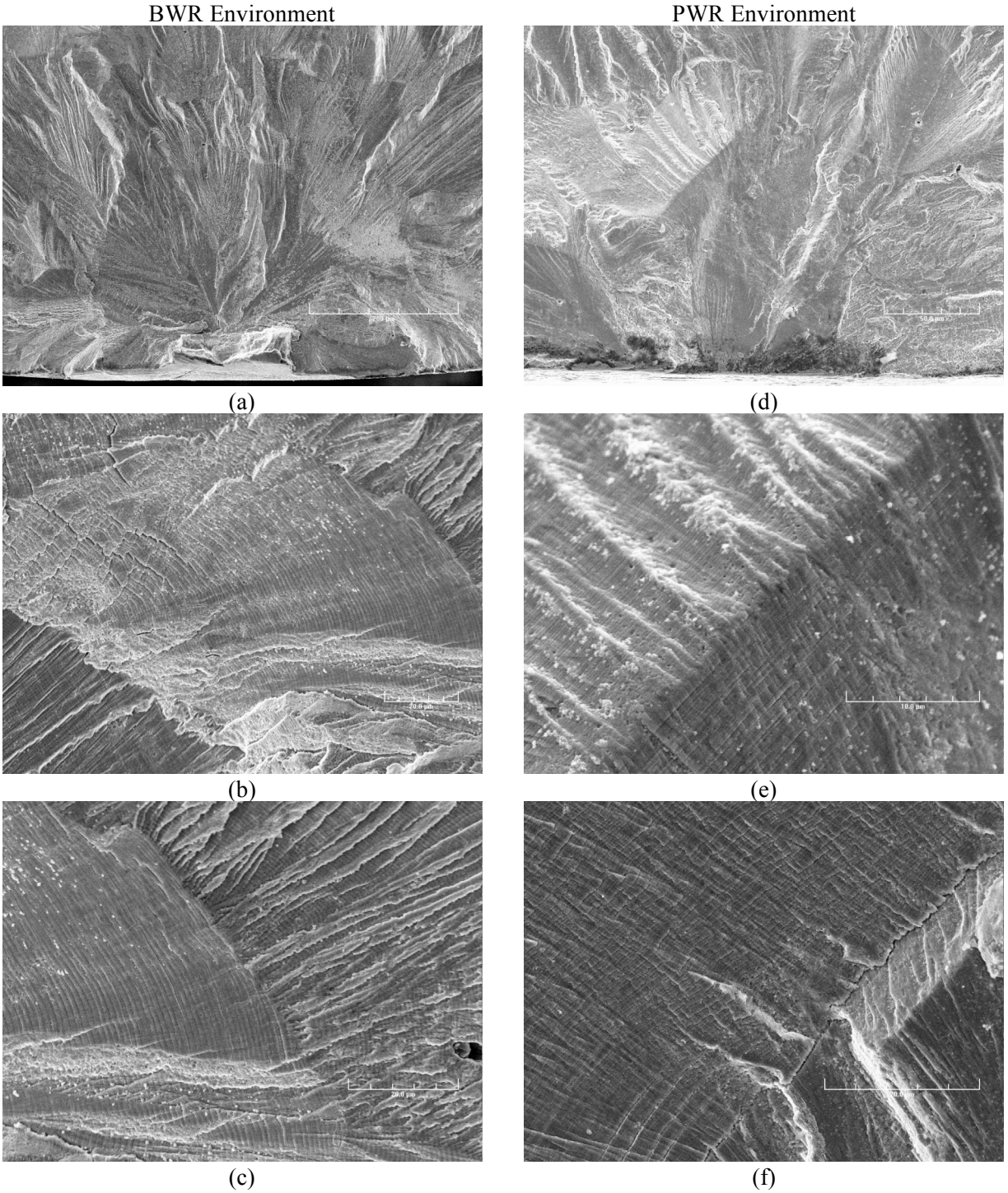

Figure 16. Photomicrographs showing crack initiation site and striations at select locations in Type 316NG SS tested in (a–c) BWR and (d–f) PWR environment.

Figure 17 presents photomicrographs that show the crack morphology in Type 316NG SS in three environments. In all cases, the tensile axis is vertical, parallel to the plane of each picture. The general appearance is that, for air tests, the cracks are more likely to be oblique, approaching 45° with respect to the tensile axis. By contrast, the cracks that formed in BWR environment appeared mixed, both oblique and normal to the tensile direction, while the cracks that formed in a PWR environment appeared mostly perpendicular to the tensile axis.

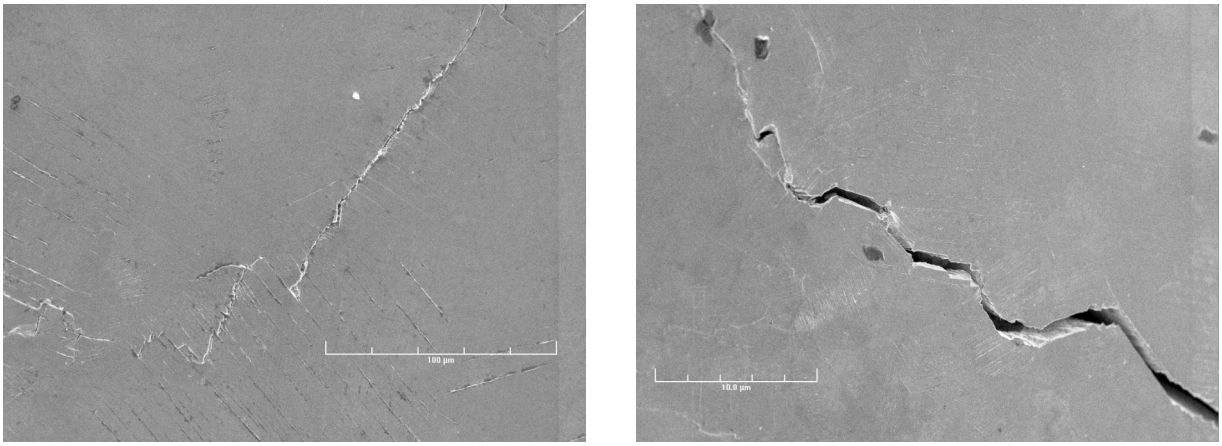

Air

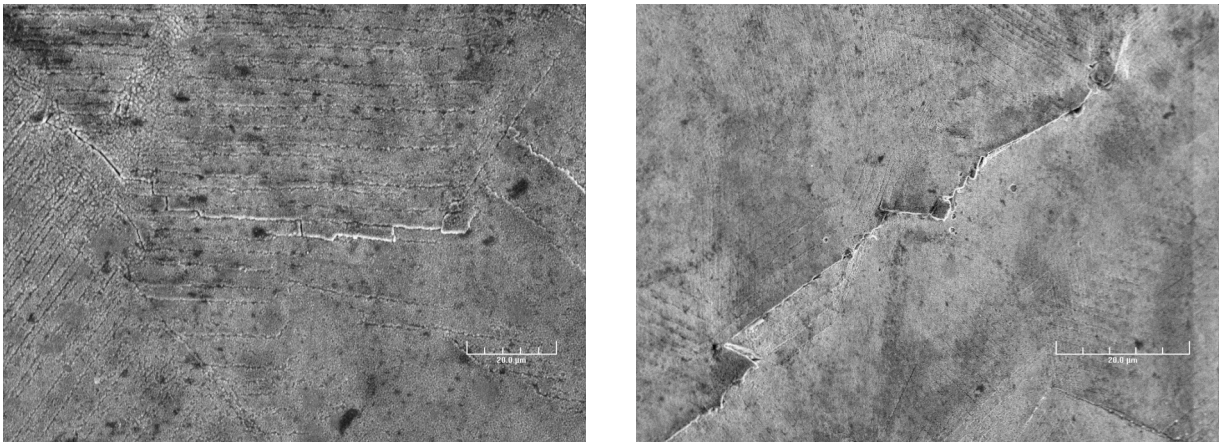

BWR Environment

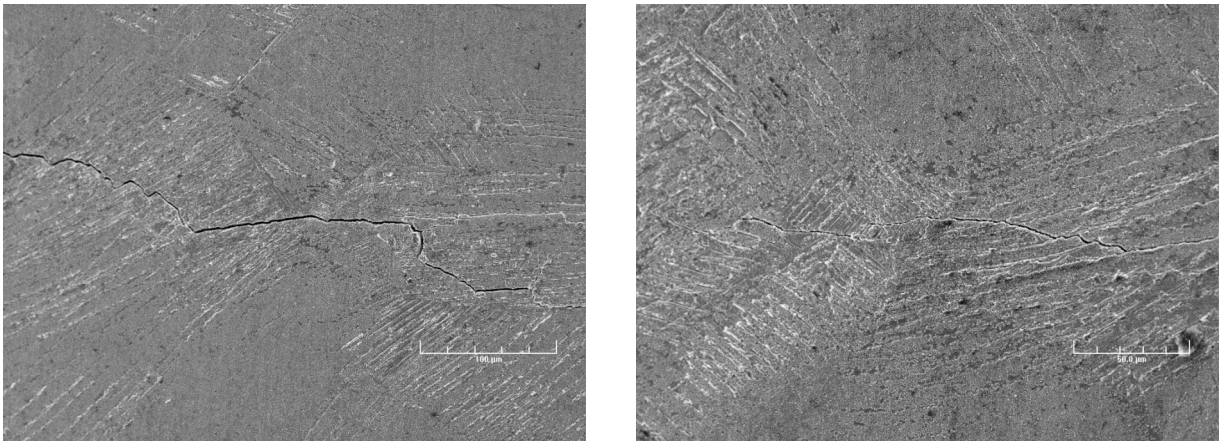

PWR Environment

Figure 17. Photomicrographs showing the morphology of lateral cracks formed in Type 316NG SS in three test environments.

4 Fatigue ε–N Data

The relevant fatigue ε–N data for austenitic SSs in air include the data compiled by Jaske and O'Donnell[16] for developing fatigue design criteria for pressure vessel alloys, the JNUFAD* database from Japan, and the results of Conway et al.[17] and Keller.[18] In water, the existing fatigue ε–N data include the tests performed by General Electric Co. (GE) in a test loop at the Dresden 1 reactor,[19] the JNUFAD database, studies at Mitsubishi Heavy Industries, Ltd. (MHI),[20–25] Ishikawajima–Harima Heavy Industries Co. (IHI),[26,27] and Hitachi[28,29] in Japan, and the present work at ANL.[4–7,30–32]

4.1 Air Environment

In an air environment, the fatigue life of Type 304 SS is comparable to that of Type 316 SS; the fatigue life of Type 316NG is slightly higher than that of Types 304 and 316 SS, particularly at high strain amplitudes. The results also indicate that the fatigue life of austenitic SSs in air is independent of temperature from room temperature to 427°C. Although the effect of strain rate on fatigue life seems to be significant at temperatures above 400°C, variations in strain rate in the range of 0.4–0.008%/s have no effect on the fatigue lives of SSs at temperatures up to 400°C.[33]

The results indicate that the Code mean curve used to develop the current Code design curve for austenitic SSs does not accurately represent the available fatigue data.[6,16] At strain amplitudes <0.5%, the mean curve predicts significantly longer lives than those observed experimentally. The difference between the Code mean curve and the best–fit of the available experimental data is due most likely to differences in the tensile strength of the steels. The Code mean curve represents SSs with relatively high strength; the fatigue ε–N data obtained during the last 30 years were obtained on SSs with lower tensile strengths. Furthermore, because, for the current Code mean curve, the value of applied stress at a fatigue life of 10^6 cycles is greater than the monotonic yield strength of austenitic SSs in more common usage, the current Code design curve for austenitic SSs does not include a mean stress correction. Studies on the effect of residual stress on fatigue life[34] indicate an apparent reduction of up to 26% in strain amplitude in the low– and intermediate–cycle regime for a mean stress of 138 MPa.

4.2 LWR Environment

The fatigue lives of austenitic SSs are decreased in LWR environments. The decrease depends primarily on applied strain amplitude, strain rate, and temperature. The results presented in Section 3.1 indicate that the effect of the DO content of the water is influenced by material heat treatment. The critical parameters that influence fatigue life, and the threshold values of these parameters for environmental effects to be significant are summarized below.

4.2.1 Strain Amplitude

A slow strain rate applied during the tensile–loading cycle (i.e., up–ramp with increasing strain) is primarily responsible for environmentally assisted reduction in fatigue life. Slow rates applied during both tensile– and compressive–loading cycles (i.e., up– and down–ramps) do not cause further decrease in fatigue life than that observed for tests with only a slow tensile–loading cycle.[30–32] Nearly all of the existing fatigue ε–N data have been obtained under loading histories with constant strain rate, temperature, and strain amplitude. Actual loading histories encountered during service of nuclear power

* M. Higuchi, Ishikawajima–Harima Heavy Industries Co., Japan, private communication to M. Prager of the Pressure Vessel Research Council, 1992.

plants are far more complex. Exploratory fatigue tests have been conducted with waveforms in which the slow strain rate is applied during only a fraction of the tensile loading cycle.[23,25] The results indicate that a minimum threshold strain is required for environmentally assisted decrease in the fatigue lives of SSs (Fig. 18). The threshold strain $\Delta\varepsilon_{th}$ appears to be independent of material type (weld or base metal) and temperature in the range of 250–325°C, but it tends to decrease as the strain amplitude is decreased.[25] The threshold strain may be expressed in terms of the applied strain range $\Delta\varepsilon$ by the equation

$$\Delta\varepsilon_{th}/\Delta\varepsilon = -0.22\ \Delta\varepsilon + 0.65. \quad (3)$$

The results suggest that the threshold strain $\Delta\varepsilon_{th}$ is related to the elastic strain range of the test, and does not correspond to the strain at which the crack closes. For fully reversed cyclic loading, the crack opening point can be identified as the point where the curvature of the load–vs.–displacement line changes before the peak compressive load is reached. In the present study, evidence of a crack opening point was observed for cracks that had grown relatively large, i.e., only near the end of life.

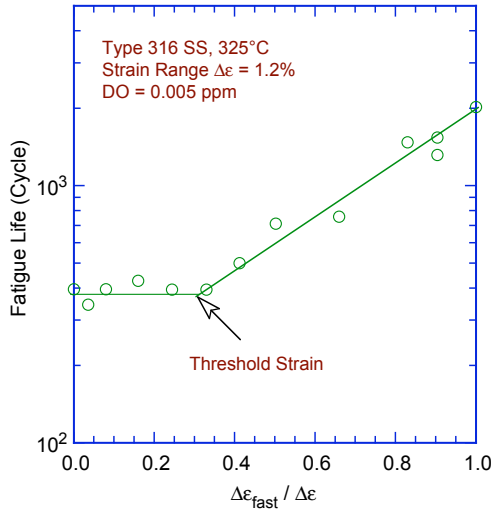

Figure 18.
Results of strain rate change tests on Type 316 SS in low–DO water at 325°C. Low strain rate was applied during only a fraction of tensile loading cycle. Fatigue life is plotted as a function of fraction of strain at high strain rate (Refs. 23, 25).

4.2.2 Hold–Time Effects

Environmental effects on fatigue life occur primarily during the tensile–loading cycle and at strain levels greater than the threshold value. Consequently, loading and environmental conditions during the tensile–loading cycle, e.g., strain rate, temperature, and DO level, are important for environmentally assisted reduction of the fatigue lives of SSs. Information about the effect of hold periods on the fatigue life of austenitic SSs in water is very limited. In high–DO water, the fatigue lives of Type 304 SS tested with a trapezoidal waveform (i.e., hold periods at peak tensile and compressive strain)[19] are comparable to those tested with a triangular waveform.[26]

4.2.3 Strain Rate

Fatigue life decreases with decreasing strain rate. In low–DO PWR environments, fatigue life decreases logarithmically with decreasing strain rate below ≈0.4%/s; the effect of environment on life saturates at ≈0.0004%/s (Fig. 19).[6,7,20–32] Only a moderate decrease in life is observed at strain rates >0.4%/s. A decrease in strain rate from 0.4 to 0.0004%/s decreases the fatigue life by a factor of ≈10.

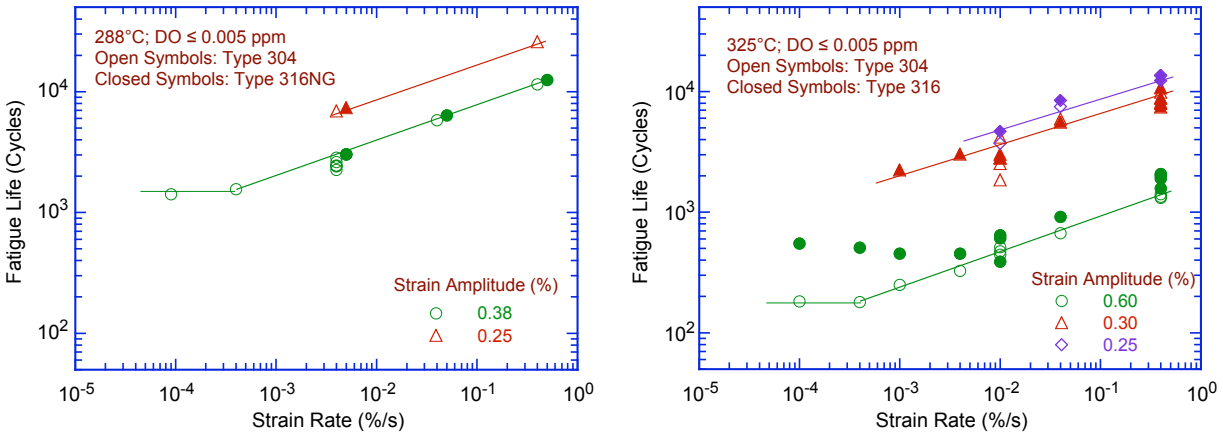

Figure 19. Dependence of fatigue lives of austenitic stainless steels on strain rate in low–DO water (Refs. 6,7).

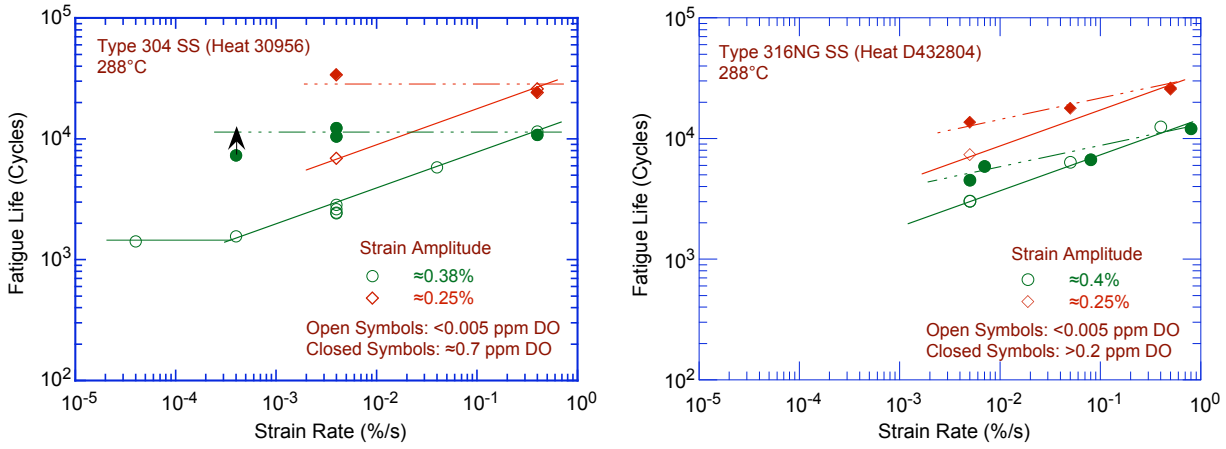

(a) (b)

Figure 20. Dependence of fatigue life of Types (a) 304 and (b) 316NG stainless steel on strain rate in high– and low–DO water at 288°C (Ref. 7).

For some SSs, the effect of strain rate may be less pronounced in high–DO water than in low–DO water (Fig. 20). For example, for Heat 30956 of Type 304 SS, strain rate has no effect on fatigue life in high–DO water, whereas life decreases linearly with strain rate in low–DO water (Fig. 20a). For Heat D432804 of Type 316NG, some effect of strain rate is observed in high–DO water, although it is smaller than that in low–DO water (Fig. 20b). These results and the effect of DO on fatigue life are discussed further in the next section. The effect of strain rate on the fatigue life of cast austenitic SSs is the same in low– and high–DO water and is comparable to that observed for the wrought SSs in low–DO water.[23,24]

4.2.4 Dissolved Oxygen

In contrast to the behavior of carbon and low–alloy steels, the fatigue lives of austenitic SSs are decreased significantly in low–DO (i.e., <0.01 ppm DO) water. The effect of environment in low–DO water is not influenced by the composition or heat treatment condition of the steel. The fatigue life continues to decrease with decreasing strain rate and increasing temperature.[6,7,22–27]

In high–DO water, the fatigue lives of austenitic SSs are either comparable to[22,24] or, in some cases, higher[6] than those in low–DO water, i.e., for some SSs, environmental effects may be lower in high– than in low–DO water. The results presented in Section 3.1 and Fig. 20a and 20b, indicate that, in high–DO water, environmental effects on the fatigue lives of austenitic SSs are influenced by the composition and heat treatment of the steel. For example, for high–carbon Type 304 SS, environmental effects are insignificant for the MA material (Fig. 20a), whereas for sensitized material the effect of environment is the same in high– and low–DO water (Fig. 5). For low–carbon Type 316NG SS some effect of strain rate is observed in high–DO water although it is smaller than that in low–DO water (Fig. 20b).

The studies at ANL indicate that, for fatigue tests in high–DO water, conductivity of water and ECP of steel are important parameters that must be maintained constant. During laboratory tests, the time to reach stable environmental conditions depends on the autoclave volume, DO level, flow rate, etc. In the ANL test facility, fatigue tests on austenitic SSs in high–DO water required a soaking period of 5–6 days for the ECP of the steel to stabilize. The steel ECP increased from zero or a negative value to above 150 mV during this period. The results shown in Fig. 20a for MA Heat 30956 of Type 304 SS in high–DO water (closed circles) were obtained on specimens that were soaked for 5–6 days before the test. The same material tested in high–DO water after soaking for only 24 h showed significant reduction in fatigue life. The results shown in Fig. 20b for Heat 432804 of Type 316NG SS in high–DO water were obtained on specimens that were soaked for only a day and therefore the ECP of the steel may not have stabilized.

To determine the possible influence of the shorter soak period, additional tests were conducted on another heat of Type 316NG (Heat P91576); these specimens were soaked for ≈10 days before testing to achieve stable values for the ECP of the steel. The results are shown in Fig. 21. Unlike the data obtained earlier on Heat D432804 (diamond symbols), the results for Heat P91576 (triangle symbols) indicate that the fatigue life of this heat is the same in low– and high–DO water. Most likely the microstructure of Heat P91576 differs from that of Heat D432804, making it more susceptible to environmental effects in high–DO water. To further investigate the effect of material microstructure on fatigue life, a specimen of Heat P91576 was solution annealed in the laboratory and tested in high–DO water at 289°C. The fatigue life of the solution–annealed specimen (inverted triangle symbol in Fig. 21) is a factor of ≈2 higher than that of the MA specimens. These results are consistent with the data presented in Section 3.1. In high–DO water, material heat treatment has a strong effect on the fatigue life of austenitic SSs.

In low–DO water, the fatigue lives of cast SSs are comparable to those of wrought SSs.[22,24] Limited data suggest that the fatigue lives of cast SSs in high–DO water are approximately the same as those in low–DO water.[6]

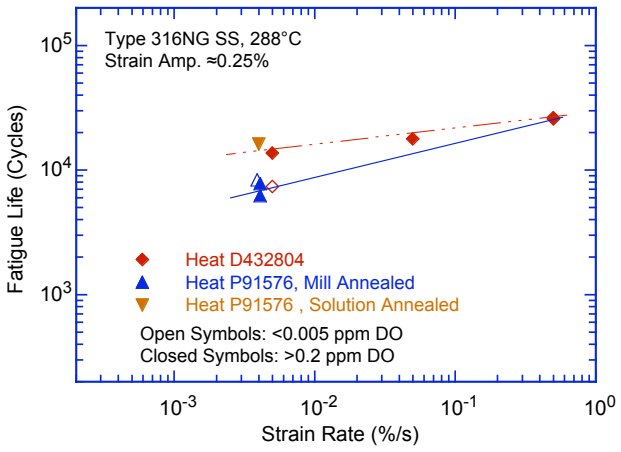

Figure 21.
Dependence of fatigue life of two heats of Type 316NG SS on strain rate in high– and low–DO water at 288°C (Ref. 5).

4.2.5 Water Conductivity

The effect of the conductivity of water and the ECP of the steel on the fatigue life of austenitic SSs is shown in Fig. 22. In high–DO water, fatigue life is decreased by a factor of ≈2 when the conductivity of water is increased from ≈0.07 to 0.4 µS/cm. Note that environmental effects appear more significant for the specimens that were soaked for only 24 h. For these tests, the ECP of steel was initially very low and increased during the test.

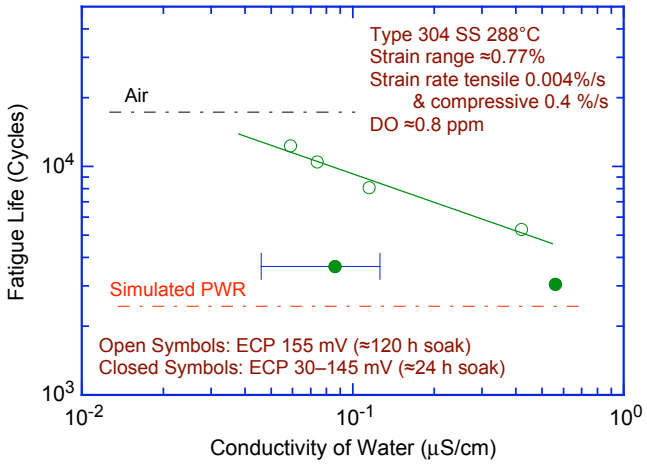

Figure 22.
Effects of conductivity of water and soaking period on fatigue life of Type 304 SS in high–DO water (Ref. 4).

4.2.6 Temperature

The change in fatigue lives of austenitic SSs with test temperature at two strain amplitudes and two strain rates is shown in Fig. 23. The results suggest a threshold temperature of 150°C, above which the environment decreases fatigue life in low–DO water if the strain rate is below the threshold of 0.4%/s. In the range of 150–325°C, the logarithm of fatigue life decreases linearly with temperature. Only moderate decrease in life is observed in water at temperatures below the threshold value of 150°C.

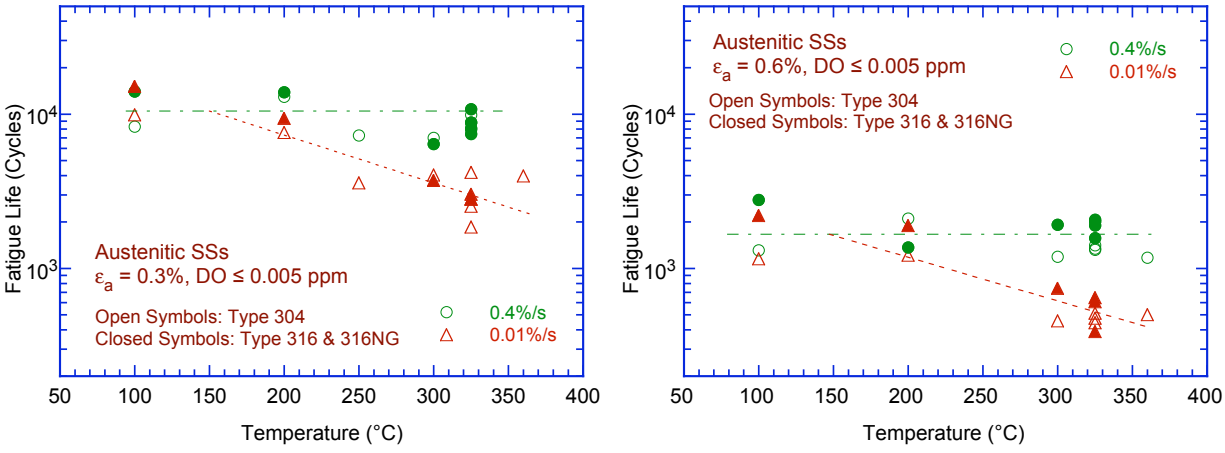

Figure 23. Change in fatigue lives of austenitic stainless steels in low–DO water with temperature (Refs. 5–7, 22–27).

Fatigue tests have been conducted at MHI in Japan on Type 316 SS under combined mechanical and thermal cycling.[23] Triangular waveforms were used for both strain and temperature cycling. Two sequences were selected for temperature cycling: an in–phase sequence, in which temperature cycling was synchronized with mechanical strain cycling; and a sequence in which temperature and strain were out of phase, i.e., maximum temperature occurred at minimum strain level and vice versa. The results are shown in Fig. 24, with the data obtained from tests at constant temperature.

For the thermal cycling tests, fatigue life should be longer for out–of–phase tests than for in–phase tests, because applied strains above the threshold strain occur at high temperatures for in–phase tests, whereas they occur at low temperatures for out–of–phase tests. An average temperature is used in Fig. 24 for the thermal cycling tests. The results from thermal cycling tests agree well with those from constant–temperature tests (open circles). The data suggest a linear decrease in the logarithm of life at temperatures above 150°C.

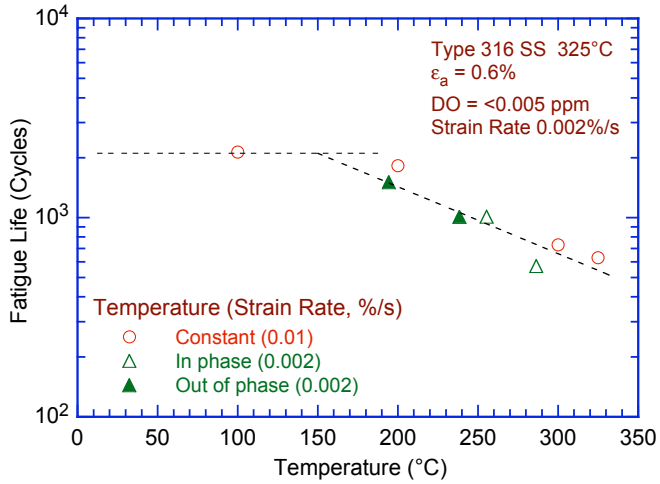

Figure 24.
Fatigue life of Type 316 stainless steel under constant and varying test temperature (Ref. 23).

4.2.7 Material Heat Treatment

The results presented in Section 3.1 (Fig. 5) indicate that, although heat treatment has little or no effect on the fatigue life of austenitic SSs in low–DO and air environments, in a high–DO environment, fatigue life may be longer for nonsensitized or slightly sensitized SS.

These results are consistent with the data obtained at MHI on solution–annealed and sensitized Types 304, 316, and 316NG SS (Figs. 25 and 26). In low–DO (<0.005 ppm) water at 325°C, a sensitization annealing has no effect on the fatigue lives of Types 304 and 316 SS (Fig. 25). However, in high–DO (8 ppm) water at 300°C, the fatigue life of sensitized Type 304 SS is a factor of ≈2 lower than that of the solution–annealed steel (Fig 26a). A sensitization anneal appears to have little or no effect on the fatigue life of Type 316NG SS in high–DO water at 288°C (Fig. 26b). Fatigue lives of solution–annealed and sensitized Type 316NG SS are comparable.

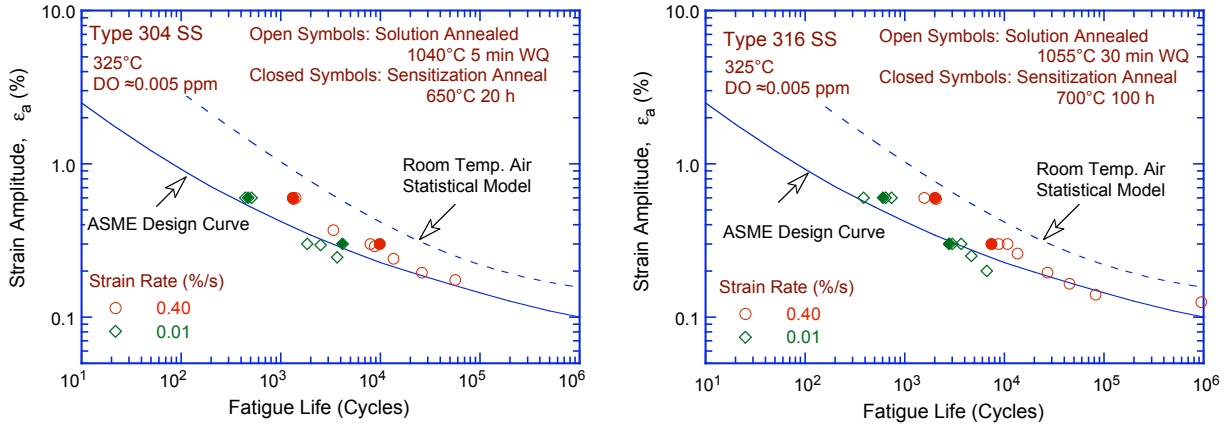

Figure 25. Effect of sensitization annealing on fatigue life of Types (a) 304 and (b) 316 stainless steel in low–DO water at 325°C (Refs. 22, 24). WQ = water quenched.

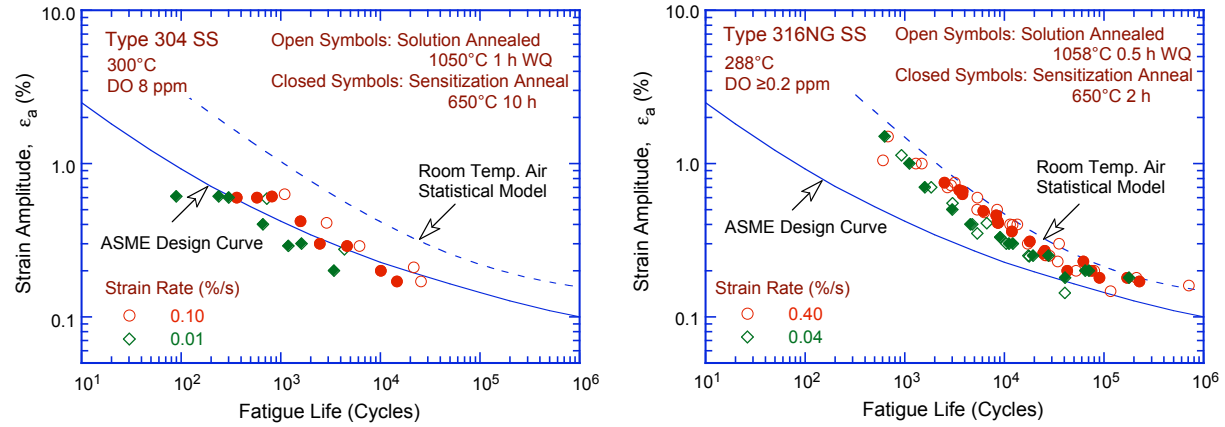

Figure 26. Effect of sensitization anneal on the fatigue lives of Types (a) 304 and (b) 316NG stainless steel in high–DO water (Refs. 20, 26). WQ = water quenched.

4.2.8 Flow Rate

It is generally recognized that flow rate most likely has a significant effect on the fatigue life of materials because it may cause differences in local environmental conditions in the enclaves of the microcracks formed during early stages in the fatigue ε–N test. Information about the effects of flow rate on the fatigue life of pressure vessel and piping steels in LWR environments has been rather limited. Recent results indicate that, under typical operating conditions for BWRs, environmental effects on the fatigue life of carbon steels are a factor of ≈2 lower at high flow rates (7 m/s) than at low flow rates (0.3 m/s or lower).[35,36] However, the effect of flow rate on the fatigue life of austenitic SSs has not been evaluated. Because the mechanism of fatigue crack initiation in austenitic SSs in LWR environments appears to be different from that in carbon and low–alloy steels, the effect of flow rate on fatigue life of SSs may also differ.

4.2.9 Surface Finish

Fatigue life is sensitive to surface finish. Cracks can initiate at surface irregularities that are normal to the stress axis. The height, spacing, shape, and distribution of surface irregularities are important for crack initiation. Fatigue tests have been conducted on Types 304 and 316NG SS specimens that were intentionally roughened in a lathe, under controlled conditions, with 5-grit sandpaper to produce circumferential cracks with an average surface roughness of 1.2 µm. The results are shown in Figs. 27a and b, respectively, for Types 316NG and 304 SS. For both steels, the fatigue life of roughened specimens is lower than that of the smooth specimens in air and low–DO water environments. In high–DO water, the fatigue life of Heat P91576 of Type 316NG is the same for rough and smooth specimens.

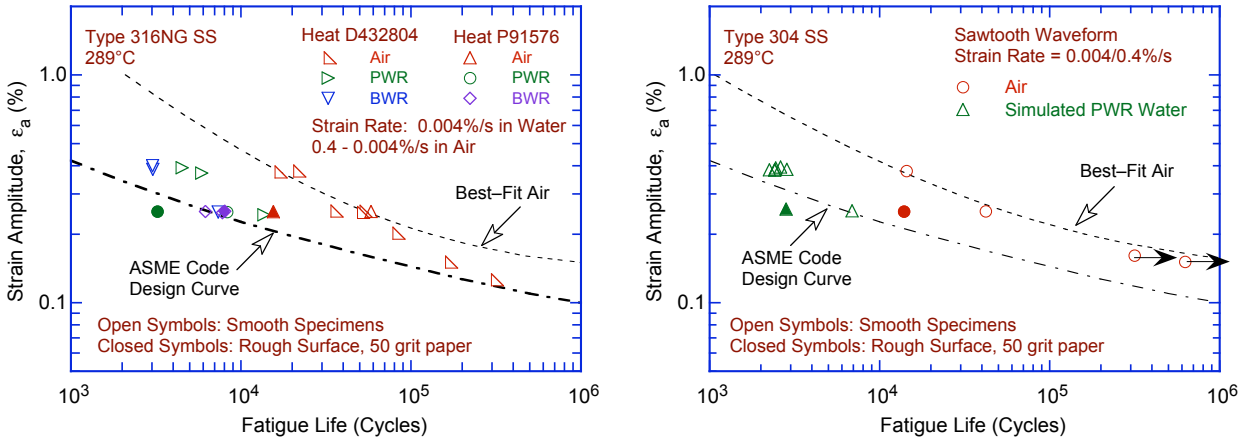

Figure 27. Effect of surface roughness on fatigue life of (a) Type 316NG and (b) Type 304 stainless steels in air and high–purity water at 289°C.

4.2.10 Cast Stainless Steels

Available fatigue ε–N data[6,22,24,32] indicate that, in air, the fatigue lives of cast CF–8 and CF–8M SSs are similar to that of wrought austenitic SSs. It is well known that the Charpy impact and fracture toughness properties of cast SSs are decreased significantly after thermal aging at temperatures between 300 and 450°C.[37–39] The cyclic–hardening behavior of cast austenitic SSs is also influenced by thermal aging.[6] At 288°C, cyclic stresses of steels aged for 10,000 h at 400°C are higher than those for unaged material or wrought SSs. Also, strain rate effects on cyclic stress are greater for aged than for unaged steel, i.e., cyclic stresses increase significantly with decreasing strain rate. The available fatigue ε–N data are inadequate to establish the effect of thermal aging on the fatigue life of cast SSs. Thermal aging may or may not affect the fatigue life.[22,24,32]

In LWR coolant environments, the fatigue lives of cast SSs are comparable to those observed for wrought SSs in low–DO water. Limited data suggest that the fatigue lives of cast SSs in high–DO water are approximately the same as those in low–DO water.[6] The results also indicate that thermal aging for 10,000 h at 400°C decreases the fatigue lives of CF8M steels.

The reduction in life in LWR environments depends on strain rate (Fig. 28). Effects of strain rate are the same in low– and high–DO water. For unaged material, environmental effects on life do not appear to saturate even at strain rates as low as 0.00001%/s.[22,24] Also, the fatigue lives of these steels are relatively insensitive to changes in ferrite content in the range of 12–28%.[22,24] Existing data are too

sparse to define the saturation strain rate for cast SSs or to establish the dependence of fatigue life on temperature in LWR environments; the effects of strain rate and temperature are assumed to be similar to those for wrought SSs.

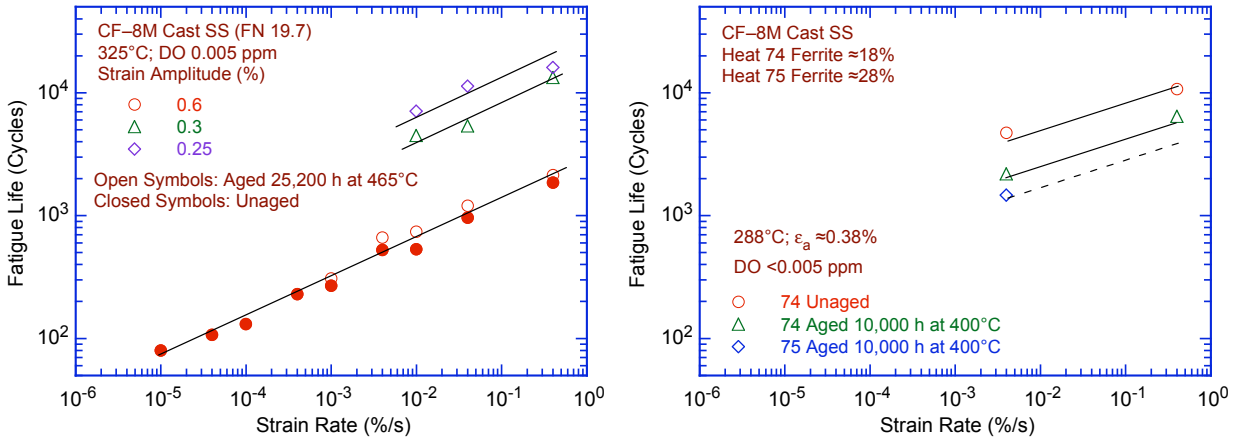

Figure 28. Dependence of fatigue lives of CF–8M cast SSs on strain rate in low–DO water at various strain amplitudes (Refs. 6,22,24,32).

5 Estimating Fatigue Life of Austenitic Stainless Steels

Several models have been developed for estimating fatigue lives of austenitic SSs in LWR environments, and the models are based on roughly the same database. Although the formulation, threshold, and saturation values of the key parameters that influence fatigue life differ, differences in the estimates of fatigue life based on these models for specific loading and environmental conditions are insignificant. Any one of these models may be used to estimate fatigue life of austenitic SSs.

5.1 ANL Statistical Model

A statistical model based on the existing fatigue ε–N data has been developed at ANL for estimating the fatigue lives of wrought and cast austenitic SSs in air and LWR environments. The model assumes that the fatigue life in air is independent of temperature and strain rate. Separate models have been developed for Type 304 or 316 SS and Type 316NG SS. In air at temperatures up to 400°C, the fatigue data for Types 304 and 316 SS are best represented by the equation:

$$\ln(N) = 6.703 - 2.030 \ln(\varepsilon_a - 0.126), \quad (4)$$

and for Type 316NG, by the equation

$$\ln(N) = 7.433 - 1.782 \ln(\varepsilon_a - 0.126). \quad (5)$$

The critical parameters that influence fatigue life and the threshold values of these parameters for environmental effects to be significant have been summarized in the previous section. In LWR environments, the fatigue life of austenitic SSs depends on strain rate, DO level, and temperature. The functional forms for the effects of strain rate and temperature were based on the data trends shown in Figs. 19 and 23, respectively. For both wrought and cast austenitic SSs, the model assumes threshold and saturation values of 0.4 and 0.0004%/s, respectively, for strain rate, and a threshold value of 150°C for temperature.

The influence of DO level on the fatigue life of austenitic SSs is not well understood. As discussed in Section 3.1, the fatigue lives of austenitic SSs are decreased significantly in low–DO water, whereas in high–DO water they are either comparable or, for some steels, higher than those in low–DO water. In high–DO water, the composition and heat treatment of the steel may influence the magnitude of environmental effects on austenitic SSs. Until more data are available to clearly establish the effects of DO level on fatigue life, the effect of DO level on fatigue life is assumed to be the same in low– and high–DO water and for wrought and cast austenitic SSs.

The least–squares fit of the experimental data in water yields a steeper slope for the ε–N curve than the slope of the curve obtained in air. These results indicate that environmental effects are more pronounced at low than at high strain amplitudes. Differing slopes for the ε–N curves in air and water environments would add complexity to the determination of the environmental correction factor F_{en}, discussed later in this paper. In the ANL statistical model, the slope of the ε–N curve is assumed to be the same in LWR and air environments. In LWR environments, fatigue data for Types 304 and 316 SS are best represented by the equation:

$$\ln(N) = 5.675 - 2.030 \ln(\varepsilon_a - 0.126) + T' \dot{\varepsilon}' O', \quad (6)$$

and that of Type 316NG, as

$$\ln(N) = 7.122 - 1.671 \ln(\varepsilon_a - 0.126) + T' \dot{\varepsilon}' O', \quad (7)$$

where T', $\dot{\varepsilon}'$, and O' are transformed temperature, strain rate, and DO, respectively, defined as follows:

$$\begin{aligned} T' &= 0 && (T < 150°C) \\ T' &= (T - 150)/175 && (150 \le T < 325°C) \\ T' &= 1 && (T \ge 325°C) \end{aligned} \quad (8)$$

$$\begin{aligned} \dot{\varepsilon}' &= 0 && (\dot{\varepsilon} > 0.4\%/s) \\ \dot{\varepsilon}' &= \ln(\dot{\varepsilon}/0.4) && (0.0004 \le \dot{\varepsilon} \le 0.4\%/s) \\ \dot{\varepsilon}' &= \ln(0.0004/0.4) && (\dot{\varepsilon} < 0.0004\%/s) \end{aligned} \quad (9)$$

$$O' = 0.281 \quad \text{(all DO levels)}. \quad (10)$$

These models are recommended for predicted fatigue lives of $\le 10^6$ cycles. Equations 6 and 8–10 should also be used for cast austenitic SSs such as CF-3, CF-8, and CF–8M. As noted earlier, because the influence of DO level on the fatigue life of austenitic SSs may be influenced by the material heat treatment, the statistical model may be somewhat conservative for some SSs in high–DO water.

5.2 Japanese MITI Guidelines

The guidelines proposed by the Japanese Ministry of International Trade and Industry (MITI), for assessing the decrease in fatigue life in LWR environments, have been presented by Higuchi et al.[40] The reduction in fatigue life of various pressure vessel and piping steels in LWR environments is expressed in terms of an environmental fatigue life correction factor F_{en}, which is the ratio of the fatigue life in air at ambient temperature to that in water at the service temperature. For austenitic SSs, F_{en} is expressed in terms of strain rate $\dot{\varepsilon}$ (%/s), temperature T (°C), and strain amplitude ε_a (%) as follows:

$$\ln(F_{en}) = (C - \dot{\varepsilon}^*) T^*, \quad (11)$$

where

$$\begin{aligned} C &= 1.182 && \text{(BWR)} \\ C &= 3.910 && \text{(PWR)} \end{aligned} \quad (12)$$

$$\begin{aligned} \dot{\varepsilon}^* &= \ln(\dot{\varepsilon}) && (0.0004 \le \dot{\varepsilon}) \\ \dot{\varepsilon}^* &= \ln(0.0004) && (\dot{\varepsilon} < 0.0004\%/s). \end{aligned} \quad (13)$$

$$\begin{aligned} T^* &= 0.000813\ T && \text{(BWR)} \\ T^* &= 0.000782\ T && \text{(PWR, } T \le 325°C) \\ T^* &= 0.254 && \text{(PWR, } T > 325°C) \end{aligned} \quad (14)$$

$$F_{en} = 1 \quad (\varepsilon_a \le 0.11\%). \quad (15)$$

The fatigue life in water is determined by dividing the life in air at ambient temperature by F_{en}. The fatigue life N in air is expressed in terms of the strain amplitude ε_a as

$$\ln(N) = 6.871 - 2.118 \ln(\varepsilon_a - 0.110). \quad (16)$$

5.3 Model Developed by the Bettis Laboratory

A model based on available fatigue ε–N data, has been developed by the Bettis Laboratory.[41] In this model, the Smith–Watson–Topper (SWT) equivalent strain parameter[42] is used to predict the fatigue life of austenitic SSs in LWR environments under prototypical temperatures and loading rates. The model indicates that the fatigue life of Type 304 SS in water depends on the temperature, strain rate, applied strain amplitude, and water oxygen level. For low–DO water, the fatigue life can be reduced by as much as a factor of 13 at high temperatures and low strain rates. The Bettis model for predicting fatigue life N in LWR environments is of the following form:

$$N = A \cdot (\varepsilon_{SWT} - \varepsilon_0)^b \cdot \left[P + (1 - P) \cdot e^{-kZ^m}\right], \tag{17}$$

where A, b, P, k, ε_0, and m are model constants, and the SWT parameter ε_{SWT} is given by

$$\varepsilon_{SWT} = (\varepsilon_a)^c \cdot \left(\frac{\sigma_{max}}{E}\right)^{1-c}, \tag{18}$$

in which maximum stress σ_{max} is the sum of the cyclic stress amplitude σ_a and mean stress σ_{mean} (i.e., = $\sigma_a + \sigma_{mean}$), E is the elastic modulus, and c is a constant determined from fatigue tests in air, in some of which a mean stress had been imposed. The effects of temperature T (K) and strain rate $\dot{\varepsilon}$ (s^{-1}) are incorporated into the model by using the Zener–Hollomon parameter Z, given by

$$Z = \dot{\varepsilon} \cdot e^{\frac{Q}{RT}}, \tag{19}$$

where R is the gas constant and Q is the fitted value of the activation energy. The model constants were determined from the existing fatigue ε–N data in water.[41] The values are as follows:*

A = 1.185 x 10^{-2} (wrought SSs, other than 316NG, in PWR water)
A = 1.185 x 10^{-2} (wrought SSs, other than 316NG, in BWR water)
b = – 2.097
ε_0 = 9.068 x 10^{-4} mm/mm
P = 0.109 (wrought SSs and welds)
c = 0.7
k = 149.0 (in PWR water)
k = 383.7 (in BWR water)
Q = 147.15 kJ/mol (35.17 kcal/mol)
R = 8.314 J/mol K (1.987 cal/mol K)
m = – 0.2233.

The cyclic stress amplitude σ_a (MPa) corresponding to a given strain amplitude ε_a (mm/mm), is obtained from the cyclic stress–vs.–strain curves in air, given by

$$\sigma_a = (175 - 0.342\ T + 7.10 \times 10^{-4}\ T^2) + (24010 - 4.54 \times 10^{-2}\ T^2 + 156\ \sigma_{mean})\ \varepsilon_a, \tag{20}$$

* T. R. Leax and D. P. Jones, Development of a Water Environment Fatigue Design Curve for Austenitic Stainless Steels, presented to ASME Subgroup on Fatigue Strength of Subcommittee Design, Sept. 24, 2002.

where T is the temperature (°C), and σ_m is the mean stress (MPa). This cyclic stress–strain curve is valid for stresses above the proportional limit. Below the proportional limit, the stress amplitude is simply the product of the elastic modulus and strain amplitude. The fatigue ε–N curve at zero mean stress can be obtained from Eqs. 17–20 by substituting a value of zero for σ_{mean} in Eqs. 18 and 20.

6 Incorporating Environmental Effects into Fatigue Evaluations

The effects of LWR coolant environments may be incorporated into the ASME Section III fatigue evaluations by either developing a new set of environmentally adjusted fatigue design curves or by using a fatigue life correction factor F_{en} to adjust the current ASME Code fatigue usage values for environmental effects. For both approaches, the magnitude of key loading and environmental parameters that influence fatigue life must be known. Estimates of fatigue life based on the two approaches may differ because of differences between the ASME mean curves used to develop the current design curves and the best–fit curves to the existing data that are used to develop the environmentally adjusted curves. However, either method provides an acceptable approach to account for environmental effects.

6.1 Fatigue Design Curves

A set of environmentally adjusted fatigue design curves may be developed from the best–fit of stress–vs.–life curves to the experimental data in LWR environments by following the procedure that was used to develop the current ASME Code fatigue design curves. The stress–vs.–life curve is obtained from the ε–N curve, e.g., stress amplitude is the product of strain amplitude and elastic modulus. The best–fit experimental curves are first adjusted for the effect of mean stress. As mentioned earlier the current ASME Code fatigue design curve for austenitic SSs does not include a mean stress correction below 10^6 cycles because, for the current Code mean curve, the fatigue strength at 10^6 cycles is greater than the monotonic yield strength of these steels. The best–fit curve in a specific environment is corrected for mean stress effects with the modified Goodman relationship given by:

$$S_a' = S_a \left(\frac{\sigma_u - \sigma_y}{\sigma_u - S_a} \right) \qquad \text{for } S_a < \sigma_y, \tag{21}$$

and

$$S_a' = S_a \qquad \text{for } S_a > \sigma_y, \tag{22}$$

where S_a' is the adjusted value of stress amplitude, and σ_y and σ_u are yield and ultimate strengths of the material, respectively. Equations 21 and 22 assume the maximum possible mean stress and typically give a conservative adjustment for mean stress, at least when environmental effects are not significant. The fatigue design curves are then obtained by lowering the adjusted best–fit curve by a factor of 2 on stress or 20 on cycles, whichever is more conservative, to account for differences and uncertainties in fatigue life that are associated with material and loading conditions. S_a'

For environmentally adjusted fatigue design curves, a minimum threshold strain is defined, below which environmental effects are insignificant. The Pressure Vessel Research Council steering committee for Cyclic Life Environmental Effects* has endorsed this threshold value and proposed a ramp for the threshold strain: a lower strain amplitude below which environmental effects are insignificant, a slightly higher strain amplitude above which environmental effects decrease fatigue life, and a ramp between the two values. The two strain amplitudes are 0.10 and 0.11% for austenitic SSs (both wrought and cast).

* Welding Research Council Progress Report, Vol. LIX No. 5/6, May/June 1999.

An example of fatigue design curves for austenitic SSs in LWR environments at 289°C is shown in Fig. 29. Because the fatigue life of Type 316NG is superior to that of Types 304 or 316 SS at high strain amplitudes, the design curves in Fig. 29 may be somewhat conservative for Type 316NG SS.

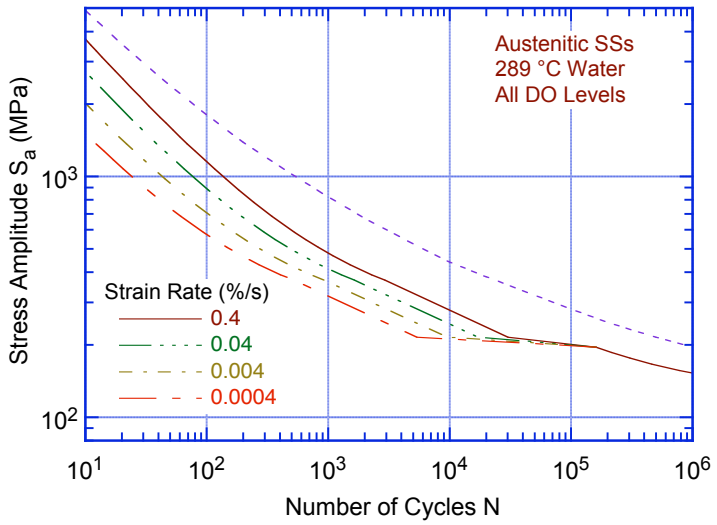

Figure 29. Fatigue design curves developed from statistical model for austenitic stainless steels in LWR environments at 289°C under service conditions where all threshold values are satisfied.

6.2 Fatigue Life Correction Factor

The effects of reactor coolant environments on fatigue life have also been expressed in terms of a fatigue life correction factor F_{en}, which is defined as the ratio of life in air at room temperature to that in water at the service temperature. Values of F_{en} can be obtained from the statistical model, where:

$$\ln(F_{en}) = \ln(N_{RTair}) - \ln(N_{water}). \quad (23)$$

The fatigue life correction factor for austenitic SSs, based on the ANL model, is given by

$$F_{en} = \exp(1.028 - T' \dot{\varepsilon}' O'), \quad (24)$$

where the constants T', $\dot{\varepsilon}'$, and O' are defined in Eqs. 8–10. F_{en} based on the MITI guidelines is given in Eqs. 11–15. To incorporate environmental effects into a Section III fatigue evaluation, the fatigue usage for a specific stress cycle, based on the current Code fatigue design curve, is multiplied by the correction factor.

7 Summary

Fatigue tests have been conducted on two heats of Type 304 SS under various material conditions to determine the effect of heat treatment on fatigue crack initiation in these steels in air and LWR environments. A detailed metallographic examination of fatigue test specimens was performed, with special attention to crack morphology at the sites of initiation, the fracture surface, and the occurrence of striations.

The results indicate that heat treatment has little or no effect on the fatigue life of Type 304 SS in air and low–DO PWR environments. In a high–DO BWR environment, fatigue life is lower for sensitized SSs; life continues to decrease as the degree of sensitization is increased. The cyclic strain–hardening behavior of Type 304 SS under various heat treatment conditions is identical, only the fatigue life varies in different environments.

In air, irrespective of the degree of sensitization, the fracture mode for crack initiation (crack lengths up to ≈200 μm) and crack propagation (crack lengths >200 μm) is transgranular (TG), most likely along crystallographic planes, leaving behind relatively smooth facets. With increasing degree of sensitization, cleavage–like or stepped TG fracture, and occasionally ridge structures on the smooth surfaces were observed. In the BWR environment, the initial crack appeared intergranular (IG) for all heat–treatment conditions, implying a weakening of the grain boundaries. For all four conditions tested, the initial IG mode transformed within 200 μm into a TG mode with cleavage–like features. It appears, however, that the size of the IG portion of the crack surface increased with the degree of sensitization. By contrast, for all of the samples tested in PWR environments, the cracks initiated and propagated in a TG mode irrespective of the degree of sensitization. Prominent features of all fracture surfaces in the PWR case were highly angular, cleavage–like fracture facets that exhibited well–defined "river" patterns. Intergranular facets were rarely observed, but when they were found, it was mostly in the more heavily sensitized alloys.

Fatigue striations normal to the crack advance direction were clearly visible beyond ≈200 μm on the fracture surfaces for all material and environmental conditions. Striations were found on both the TG and IG facets of the samples tested in BWR conditions, or co-existing with the "river" patterns specific to the samples tested in the PWR environment. Evidence of extensive rubbing due to repeated contact between the two mating surfaces was also found.

The orientation of the cracks as they initiated at the specimen surface was also a function of the test environment. For air tests, cracks initiated obliquely, approaching 45°, with respect to the tensile axis. By contrast, for tests in either BWR or PWR environment cracks tended to initiate perpendicular to the tensile axis. In all environments, the overall orientation of the crack became perpendicular to the tensile axis as the crack grew beyond the initiation stage.

In air, the fatigue lives of Types 304 and 316 SS are comparable; those of Type 316NG are superior to those of Types 304 and 316 SS at high strain amplitudes. The fatigue lives of austenitic SSs in air are independent of temperature in the range from room temperature to 427°C. Also, variation in strain rate in the range of 0.4–0.008%/s has no effect on the fatigue lives of SSs at temperatures up to 400°C. The fatigue ε–N behavior of cast SSs is similar to that of wrought austenitic SSs.

Review of the available data show that the fatigue lives of cast and wrought austenitic SSs are decreased in LWR environments; the decrease depends on strain rate, DO level in water, and temperature.

A minimum threshold strain is required for environmentally assisted decrease in the fatigue life of SSs, and this strain appears to be independent of material type (weld or base metal) and temperature in the range of 250–325°C. Environmental effects on fatigue life occur primarily during the tensile–loading cycle and at strain levels greater than the threshold value. Strain rate and temperature have a strong effect on fatigue life in LWR environments. Fatigue life decreases logarithmically with decreasing strain rate below 0.4%/s. The effect saturates at 0.0004%/s. Similarly, the fatigue ε–N data suggest a threshold temperature of 150°C; in the range of 150–325°C, the logarithm of life decreases linearly with temperature.

The fatigue lives of wrought and cast austenitic SSs are decreased significantly in low–DO (i.e., <0.01 ppm DO) water. In these environments, the composition or heat treatment of the steel has little or no effect on fatigue life. However, in high–DO water the environmental effects on fatigue life are influenced by the composition and heat treatment of the steel. For a high–carbon heat of Type 304 SS, environmental effects were significant only for the sensitized steel. For a low–carbon heat of Type 316NG SS, some effect of environment was observed even for MA steel in high–DO water, although the effect was smaller than that observed in low–DO water. Limited fatigue ε–N data indicate that the fatigue lives of cast SSs are approximately the same in low– and high–DO water and are comparable to those observed for wrought SSs in low–DO water.

Statistical models for the fatigue life of austenitic SSs as a function of material, loading, and environmental parameters have been developed. The functional form of the model and bounding values of the important parameters are based on experimental observations and data trends. The models are recommended for predicted fatigue lives of $\leq 10^6$ cycles. Consistent with previous work by Jaske and O'Donnell, the present results indicate that even in air the ASME mean curve for SSs is not consistent with the experimental data. The ASME curve is nonconservative. The results that correspond to the 50th percentile of the statistical model are considered to be the best fit to the experimental data.

Two approaches are presented for incorporating the effects of LWR environments into ASME Section III fatigue evaluations**.** In the first approach, environmentally adjusted fatigue design curves are developed by adjusting the best–fit experimental curve for the effect of mean stress and by setting margins of 20 on cycles and 2 on strain to account for the uncertainties in life associated with material and loading conditions. These curves provide allowable cycles for fatigue crack initiation in LWR coolant environments. The second approach considers the effects of reactor coolant environments on fatigue life in terms of an environmental correction factor F_{en}, which is the ratio of fatigue life in air at room temperature to that in water under reactor operating conditions. To incorporate environmental effects into the ASME Code fatigue evaluations, a fatigue usage factor for a specific load set, based on the current Code design curves, is multiplied by the correction factor.

References

1. Langer, B. F., "Design of Pressure Vessels for Low–Cycle Fatigue," ASME J. Basic Eng. 84, 389–402, 1962.

2. Criteria of Section III of the ASME Boiler and Pressure Vessel Code for Nuclear Vessels, The American Society of Mechanical Engineers, New York, 1964.

3. Chopra, O. K., and W. J. Shack, "Effects of LWR Coolant Environments on Fatigue Design Curves of Carbon and Low–Alloy Steels," NUREG/CR–6583, ANL–97/18, March 1998.

4. Chopra, O. K., and W. J. Shack, "Environmental Effects on Fatigue Crack Initiation in Piping and Pressure Vessel Steels," NUREG/CR–6717, ANL–00/27, May 2001.

5. Chopra, O. K., and W. J. Shack, "Review of the Margins for ASME Code Design Curves – Effects of Surface Roughness and Material Variability," NUREG/CR–6815, ANL–02/39, Sept. 2003.

6. Chopra, O. K., "Effects of LWR Coolant Environments on Fatigue Design Curves of Austenitic Stainless Steels," NUREG/CR–5704, ANL–98/31, 1999.

7. Chopra, O. K., "Mechanisms and Estimation of Fatigue Crack Initiation in Austenitic Stainless Steels in LWR Environments," NUREG/CR–6787, ANL–01/25, Aug. 2002.

8. Majumdar, S., O. K. Chopra, and W. J. Shack, "Interim Fatigue Design Curves for Carbon, Low–Alloy, and Austenitic Stainless Steels in LWR Environments," NUREG/CR–5999, ANL–93/3, 1993.

9. Keisler, J., O. K. Chopra, and W. J. Shack, "Fatigue Strain–Life Behavior of Carbon and Low–Alloy Steels, Austenitic Stainless Steels, and Alloy 600 in LWR Environments," NUREG/CR–6335, ANL–95/15, 1995.

10. Higuchi, M., and K. Iida, "Fatigue Strength Correction Factors for Carbon and Low–Alloy Steels in Oxygen–Containing High–Temperature Water," Nucl. Eng. Des. 129, 293–306, 1991.

11. Iida, K., T. Bannai, M. Higuchi, K. Tsutsumi, and K. Sakaguchi, "Comparison of Japanese MITI Guideline and Other Methods for Evaluation of Environmental Fatigue Life Reduction," in Pressure Vessel and Piping Codes and Standards, PVP Vol. 419, M. D. Rana, ed., American Society of Mechanical Engineers, New York, pp. 73–81, 2001.

12. Park, J. Y., and W. J. Shack, "Intergranular Crack Propagation Rates in Sensitized Type 304 Stainless Steel in an Oxygenated Water Environment," ANL–83–93, Dec. 1983.

13. Ruther, W. E., W. K. Soppet, and T. F. Kassner, "Evaluation of Environmental Corrective Actions," in Materials Science and Technology Division Light–Water–Reactor Safety Research Program: Quarterly Progress Report, October–December 1983, NUREG/CR–3689 Vol. IV, ANL–83–85 Vol. IV, pp. 51–57, Aug. 1984.

14. Macdonald, D. D., A. C. Scott, and P. Wentrcek, "External Reference Electrodes for Use in High Temperature Aqueous Systems," J. Electrochem. Soc. 126, 908–911, 1979.

15. Smith, J. L., O. K. Chopra, and W. J. Shack, "Effect of Water Chemistry on the Fatigue Life of Austenitic Stainless Steels in LWR Environments," in Environmentally Assisted Cracking in Light Water Reactors, Semiannual Report, January 1999–June 1999, NUREG/CR–4667, Vol. 28, ANL–00/7, pp. 13–27, July 2000.

16. Jaske, C. E., and W. J. O'Donnell, "Fatigue Design Criteria for Pressure Vessel Alloys," Trans. ASME J. Pressure Vessel Technol. 99, 584–592, 1977.

17. Conway, J. B., R. H. Stentz, and J. T. Berling, "Fatigue, Tensile, and Relaxation Behavior of Stainless Steels," TID–26135, U.S. Atomic Energy Commission, Washington, DC, 1975.

18. Keller, D. L., "Progress on LMFBR Cladding, Structural, and Component Materials Studies During July, 1971 through June, 1972, Final Report," Task 32, Battelle–Columbus Laboratories, BMI–1928, 1977.

19. Hale, D. A., S. A. Wilson, E. Kiss, and A. J. Gianuzzi, "Low–Cycle Fatigue Evaluation of Primary Piping Materials in a BWR Environment," GEAP–20244, U.S. Nuclear Regulatory Commission, Sept. 1977.

20. Fujiwara, M., T. Endo, and H. Kanasaki, "Strain Rate Effects on the Low–Cycle Fatigue Strength of 304 Stainless Steel in High–Temperature Water Environment; Fatigue Life: Analysis and Prediction," in Proc. Intl. Conf. and Exposition on Fatigue, Corrosion Cracking, Fracture Mechanics, and Failure Analysis, ASM, Metals Park, OH, pp. 309–313, 1986.

21. Mimaki, H., H. Kanasaki, I. Suzuki, M. Koyama, M. Akiyama, T. Okubo, and Y. Mishima, "Material Aging Research Program for PWR Plants," in Aging Management Through Maintenance Management, PVP Vol. 332, I. T. Kisisel, ed., American Society of Mechanical Engineers, New York, pp. 97–105, 1996.

22. Kanasaki, H., R. Umehara, H. Mizuta, and T. Suyama, "Fatigue Lives of Stainless Steels in PWR Primary Water," Trans. 14th Intl. Conf. on Structural Mechanics in Reactor Technology (SMiRT 14), Lyon, France, pp. 473–483, 1997.

23. Kanasaki, H., R. Umehara, H. Mizuta, and T. Suyama, "Effects of Strain Rate and Temperature Change on the Fatigue Life of Stainless Steel in PWR Primary Water," Trans. 14th Intl. Conf. on Structural Mechanics in Reactor Technology (SMiRT 14), Lyon, France, pp. 485–493, 1997.

24. Tsutsumi, K., H. Kanasaki, T. Umakoshi, T. Nakamura, S. Urata, H. Mizuta, and S. Nomoto, "Fatigue Life Reduction in PWR Water Environment for Stainless Steels," in Assessment Methodologies for Preventing Failure: Service Experience and Environmental Considerations, PVP Vol. 410-2, R. Mohan, ed., American Society of Mechanical Engineers, New York, pp. 23–34, 2000.

25. Tsutsumi, K., T. Dodo, H. Kanasaki, S. Nomoto, Y. Minami, and T. Nakamura, "Fatigue Behavior of Stainless Steel under Conditions of Changing Strain Rate in PWR Primary Water," in Pressure Vessel and Piping Codes and Standards, PVP Vol. 419, M. D. Rana, ed., American Society of Mechanical Engineers, New York, pp. 135–141, 2001.

26. Higuchi, M., and K. Iida, "Reduction in Low–Cycle Fatigue Life of Austenitic Stainless Steels in High–Temperature Water," in Pressure Vessel and Piping Codes and Standards, PVP Vol. 353, D. P. Jones, B. R. Newton, W. J. O'Donnell, R. Vecchio, G. A. Antaki, D. Bhavani, N. G. Cofie, and G. L. Hollinger, eds., American Society of Mechanical Engineers, New York, pp. 79–86, 1997.

27. Higuchi, M., K. Iida, and K. Sakaguchi, "Effects of Strain Rate Fluctuation and Strain Holding on Fatigue Life Reduction for LWR Structural Steels in Simulated PWR Water," in Pressure Vessel and Piping Codes and Standards, PVP Vol. 419, M. D. Rana, ed., American Society of Mechanical Engineers, New York, pp. 143–152, 2001.

28. Hayashi, M., "Thermal Fatigue Strength of Type 304 Stainless Steel in Simulated BWR Environment," Nucl. Eng. Des. 184, 135–144, 1998.

29. Hayashi, M., K. Enomoto, T. Saito, and T. Miyagawa, "Development of Thermal Fatigue Testing with BWR Water Environment and Thermal Fatigue Strength of Austenitic Stainless Steels," Nucl. Eng. Des. 184, 113–122, 1998.

30. Chopra, O. K., and D. J. Gavenda, "Effects of LWR Coolant Environments on Fatigue Lives of Austenitic Stainless Steels," in Pressure Vessel and Piping Codes and Standards, PVP Vol. 353, D. P. Jones, B. R. Newton, W. J. O'Donnell, R. Vecchio, G. A. Antaki, D. Bhavani, N. G. Cofie, and G. L. Hollinger, eds., American Society of Mechanical Engineers, New York, pp. 87–97, 1997.

31. Chopra, O. K., and D. J. Gavenda, "Effects of LWR Coolant Environments on Fatigue Lives of Austenitic Stainless Steels," J. Pressure Vessel Technol. 120, 116–121, 1998.

32. Chopra, O. K., and J. L. Smith, "Estimation of Fatigue Strain–Life Curves for Austenitic Stainless Steels in Light Water Reactor Environments," in Fatigue, Environmental Factors, and New Materials, PVP Vol. 374, H. S. Mehta, R. W. Swindeman, J. A. Todd, S. Yukawa, M. Zako, W. H. Bamford, M. Higuchi, E. Jones, H. Nickel, and S. Rahman, eds., American Society of Mechanical Engineers, New York, pp. 249–259, 1998.

33. Amzallag, C., P. Rabbe, G. Gallet, and H.–P. Lieurade, "Influence des Conditions de Sollicitation Sur le Comportement en Fatigue Oligocyclique D'aciers Inoxydables Austénitiques," Memoires Scientifiques Revue Metallurgie Mars, pp. 161–173, 1978.

34. Wire, G. L., T. R. Leax, and J. T. Kandra, "Mean Stress and Environmental Effects on Fatigue in Type 304 Stainless Steel," in Probabilistic and Environmental Aspects of Fracture and Fatigues, PVP Vol. 386, S. Rahman, ed., American Society of Mechanical Engineers, New York, pp. 213–228, 1999.

35. Hirano, A., M. Yamamoto, K. Sakaguchi, K. Iida, and T. Shoji, "Effects of Water Flow Rate on Fatigue Life of Carbon Steel in High–Temperature Pure Water Environment," in Assessment Methodologies for Predicting Failure: Service Experience and Environmental Considerations, PVP Vol. 410–2, R. Mohan, ed., American Society of Mechanical Engineers, New York, pp. 13–18, 2000.

36. Lenz, E., N. Wieling, and H. Muenster, "Influence of Variation of Flow Rates and Temperature on the Cyclic Crack Growth Rate under BWR Conditions," in Environmental Degradation of Materials in Nuclear Power Systems – Water Reactors, The Metallurgical Society, Warrendale, PA, 1988.

37. Slama, G., P. Petrequin, and T. Mager, "Effect of Aging on Mechanical Properties of Austenitic Stainless Steel Castings and Welds," in Assuring Structural Integrity of Steel Reactor Pressure Boundary Components, SMiRT Post Conference Seminar 6, Monterey, CA, 1983.

38. Chopra, O. K., "Estimation of Fracture Toughness of Cast Stainless Steels During Thermal Aging in LWR Systems," NUREG/CR–4513, ANL–93/22, Aug. 1994.

39. Chopra, O. K., "Effect of Thermal Aging on Mechanical Properties of Cast Stainless Steels," in Proc. of the 2nd Int. Conf. on Heat–Resistant Materials, K. Natesan, P. Ganesan, and G. Lai, eds., ASM International, Materials Park, OH, pp. 479–485, 1995.

40. Higuchi, M., K. Iida, A. Hirano, K. Tsutsumi, and K. Sakaguchi, "A Proposal of Fatigue Life Correlation Factor F_{en} for Austenitic Stainless Steels in LWR Water Environments," in Pressure Vessel and Piping Codes and Standards – 2002, PVP Vol. 439, M. D. Rana, ed., American Society of Mechanical Engineers, New York, pp. 109–117, 2002.

41. Leax, T. R., "Statistical Models of Mean Stress and Water Environment Effects on the Fatigue Behavior of 304 Stainless Steel," in Probabilistic and Environmental Aspects of Fracture and Fatigues, PVP Vol. 386, S. Rahman, ed., American Society of Mechanical Engineers, New York, pp. 229–239, 1999.

42. Smith, K. N., P. Watson, and T. H. Topper, "A Stress–Strain Function for the Fatigue of Metals," J. Mater., JMLSA 5 (4), 767–778, 1970.

NRC FORM 335
(2–89)
NRCM 1102,
3201, 3202

U. S. NUCLEAR REGULATORY COMMISSION

BIBLIOGRAPHIC DATA SHEET

(See instructions on the reverse)

1. REPORT NUMBER
(Assigned by NRC. Add Vol., Supp., Rev., and Addendum Numbers, if any.)

NUREG/CR–6878
ANL–03/35

2. TITLE AND SUBTITLE

Effect of Material Heat Treatment on Fatigue Crack Initiation in Austenitic Stainless Steels in LWR Environments

3. DATE REPORT PUBLISHED

MONTH	YEAR
July	2005

4. FIN OR GRANT NUMBER

Y6388

5. AUTHOR(S)

O. K. Chopra, B. Alexandreanu, and W. J. Shack

6. TYPE OF REPORT

Technical

7. PERIOD COVERED (Inclusive Dates)

8. PERFORMING ORGANIZATION – NAME AND ADDRESS (If NRC, provide Division, Office or Region, U.S. Nuclear Regulatory Commission, and mailing address; if contractor, provide name and mailing address.)

Argonne National Laboratory
9700 South Cass Avenue
Argonne, IL 60439

9. SPONSORING ORGANIZATION – NAME AND ADDRESS *(If NRC, type "Same as above": if contractor, provide NRC Division, Office or Region, U.S. Nuclear Regulatory Commission, and mailing address.)*

Division of Engineering Technology
Office of Nuclear Regulatory Research
U.S. Nuclear Regulatory Commission
Washington, DC 20555–0001

10. SUPPLEMENTARY NOTES

William H. Cullen, Jr., NRC Project Manager

11. ABSTRACT (200 words or less)

The ASME Boiler and Pressure Vessel Code provides rules for the design of Class 1 components of nuclear power plants. Figures I–9.1 through I–9.6 of Appendix I to Section III of the Code specify design curves for applicable structural materials. However, the effects of light water reactor (LWR) coolant environments are not explicitly addressed by the Code design curves. The existing fatigue strain–vs.–life (ε–N) data illustrate potentially significant effects of LWR coolant environments on the fatigue resistance of pressure vessel and piping steels. Under certain environmental and loading conditions, fatigue lives of austenitic stainless steels (SSs) can be a factor of 20 lower in water than in air. This report presents experimental data on the effect of heat treatment on fatigue crack initiation in austenitic Type 304 SS in LWR coolant environments. A detailed metallographic examination of fatigue test specimens was performed to characterize the crack morphology and fracture morphology. The key material, loading, and environmental parameters and their effect on the fatigue life of these steels are also described. Statistical models are presented for estimating the fatigue ε–N curves for austenitic SSs as a function of material, loading, and environmental parameters. Two methods for incorporating the effects of LWR coolant environments into the ASME Code fatigue evaluations are presented.

12. KEY WORDS/DESCRIPTORS *(List words or phrases that will assist researchers in locating this report.)*

Fatigue Strain–Life Curves
Fatigue Design Curves
Fatigue Crack Initiation
LWR Environment
Austenitic Stainless Steels
Cast Austenitic Stainless Steels

13. AVAILABILITY STATEMENT

Unlimited

14. SECURITY CLASSIFICATION

(This Page)
Unclassified

(This Report)
Unclassified

15. NUMBER OF PAGES

16.ICE PR

NRC FORM 335 (2–89)